AD-A105 871 NAVAL SURFACE WEAPONS CENTER SILVER SPRING MD F/G 17/9
DEVELOPMENT AND TESTING OF A MILLIMETER WAVE MONOPULSE TRACKING--ETC(U)
JUL 80 N DEMINCO, D D BRICKERD, C G PAYNE
UNCLASSIFIED NSWC/TR-80-397 NL

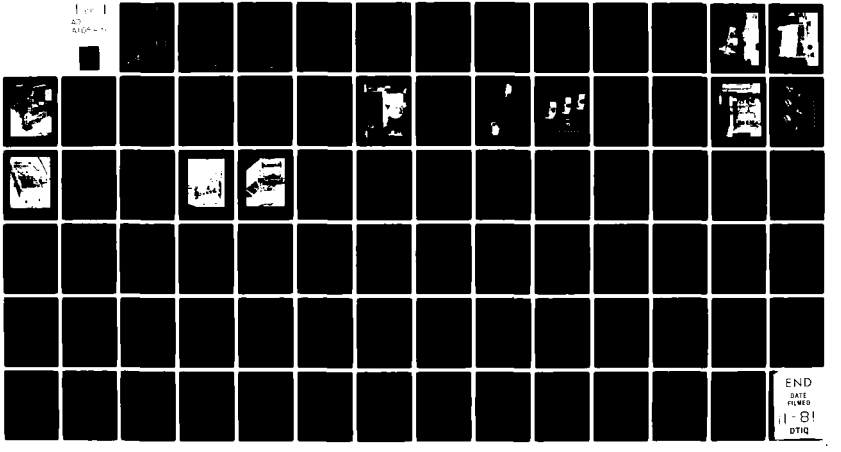

END
DATE FILMED
11-81
DTIC

(12) LEVEL II

NSWC TR 80-397

DEVELOPMENT AND TESTING OF A MILLIMETER WAVE MONOPULSE TRACKING RADAR

BY N. DeMINCO C. G. PAYNE D. D. BRICKERD W. J. KOURY

ELECTRONICS SYSTEMS DEPARTMENT

JULY 1980

Approved for public release, distribution unlimited.

NAVAL SURFACE WEAPONS CENTER

Dahlgren, Virginia 22448 • Silver Spring, Maryland 20910

UNCLASSIFIED

SECURITY CLASSIFICATION OF THIS PAGE (When Data Entered)

REPORT DOCUMENTATION PAGE	READ INSTRUCTIONS BEFORE COMPLETING FORM
1. REPORT NUMBER: 14 NSWC/TR-80-397 | 2. GOVT ACCESSION NO.: AD-A105871	3. RECIPIENT'S CATALOG NUMBER:
4. TITLE (and Subtitle): DEVELOPMENT AND TESTING OF A MILLIMETER WAVE MONOPULSE TRACKING RADAR,	5. TYPE OF REPORT & PERIOD COVERED: Final 1974 - 1980
	6. PERFORMING ORG. REPORT NUMBER:
7. AUTHOR(s): N. DeMinco, C. G. Payne, D. D. Brickerd, W. J. Koury	8. CONTRACT OR GRANT NUMBER(s): N1F32-111
9. PERFORMING ORGANIZATION NAME AND ADDRESS: Naval Surface Weapons Center, White Oak, Silver Spring, MD 20910	10. PROGRAM ELEMENT, PROJECT, TASK AREA & WORK UNIT NUMBERS: Sub-project No. SP32-399-491
11. CONTROLLING OFFICE NAME AND ADDRESS	12. REPORT DATE: July 1980 (11) 81 13. NUMBER OF PAGES: 86
14. MONITORING AGENCY NAME & ADDRESS (if different from Controlling Office)	15. SECURITY CLASS. (of this report): UNCLASSIFIED 15a. DECLASSIFICATION/DOWNGRADING SCHEDULE:

16. DISTRIBUTION STATEMENT (of this Report)

Approved for public release, distribution unlimited.

17. DISTRIBUTION STATEMENT (of the abstract entered in Block 20, if different from Report)

18. SUPPLEMENTARY NOTES

19. KEY WORDS (Continue on reverse side if necessary and identify by block number)

20. ABSTRACT (Continue on reverse side if necessary and identify by block number)

This report describes the development, theoretical analysis, testing, and test results of a 35-GHz Monopulse Tracking Radar. A rationale is given as to why a radar at this frequency is beneficial to Navy weapons systems. The specific area addressed is the tracking of air targets at low elevation angles. This report contains a detailed description of all of the subsystems of the radar, a theoretical prediction of system performance, a discussion of the low angle tracking problem, the problems encountered in the development of the

DD FORM 1 JAN 73 1473 EDITION OF 1 NOV 65 IS OBSOLETE
S/N 0102-LF-014-6601

UNCLASSIFIED
SECURITY CLASSIFICATION OF THIS PAGE (When Data Entered)

411 043

20. Abstract (Cont'd)

radar, the test program, and the results of that test program. All work was funded as part of the Center's Independent Exploratory Development program.

FOREWORD

This report describes the development, theoretical analysis, testing, and test results of a 35-GHz Monopulse Tracking Radar. A rationale is given as to why a radar at this frequency is beneficial to Navy weapons systems. The specific area addressed is the tracking of air targets at low elevation angles. This report contains a detailed description of all of the subsystems of the radar, a theoretical prediction of system performance, a discussion of the low angle tracking problem, the problems encountered in the development of the radar, the test program, and the results of that test program. All work was funded as part of the Center's Independent Exploratory Development program.

This report has been reviewed by Donald L. Wilson, Radar Development Group Head; T. C. Pendergraft, Radar Engineering Branch Head; and J. R. Pollard, Electromagnetic Systems Division Head.

Released by:

DAVID B. COLBY, Head
Electronics Systems Department

CONTENTS

ILLUSTRATIONS

ILLUSTRATIONS (Cont'd)

TABLES

INTRODUCTION

The Radar Engineering Branch (F46) of the Naval Surface Weapons Center (NSWC) has developed a millimeter wave tracking radar to evaluate potential shipboard applications for low angle target tracking and surveillance. The improvements in millimeter wavelength components have made it possible to construct a high power monopulse tracking radar at 35 GHz. A test program was completed during the first quarter of FY 80 which measured the significant performance characteristics of the radar. This report describes the radar, the theoretical analysis of the radar system, the problems encountered in the development and testing of the system, the test program, and the test results.

Radars operating in the millimeter wave frequency region have certain inherent advantages in tracking and guidance systems when compared to radars in the microwave and infrared regions. Some of these advantages are: high antenna gain (and hence good angular resolution) with physically small apertures; atmospheric absorption bands for low probability of intercept electronic counter-countermeasures; increased immunity in an electronic countermeasures (ECM) environment (stand off jamming); inherent electromagnetic compatibility; physically small components, even in waveguide, which offer packaging and weight advantages; and all weather and day/night capability.

Results of the 35-GHz millimeter wave radar performance tests indicate this type of radar could fulfill the low angle tracking requirements of the surface Navy.

SYSTEM DESCRIPTION

BASIC SYSTEM DESCRIPTION

The radar developed at NSWC represents the present state-of-the-art in components at 35 GHz. Table 1 is a list of the millimeter wave system parameters. Availability of state-of-the-art hardware plus system performance requirements determined these system parameters. In particular, critical millimeter wave components include a high power waveguide duplexer (containing latching ferrite and differential phase shift circulators), low-noise figure [5.0-dB double sideband (DSB)] Schottky diode mixers, a Cassegrain monopulse antenna, an all solid state transmitter modulator, and a long life inverted coaxial magnetron. These components are all shown schematically in the block diagram of the system (see Figure 1). Each component of this block diagram will be discussed in detail in this report.

Table 1. Radar Systems Parameters

Parameter	Value
Transmitter Type	Coaxial Magnetron
Operating Frequency	35 GHz
Peak Transmitting Power	100 kW
Pulsewidth	0.1, 0.5, 1.0 μsec
Pulse Repetition Frequency	5.5, 1.1, 0.55 KPPS
Average Power	5.5 W
Antenna Gain	43 dB
Beamwidth	1°
Polarization	Vert., Horz., Circular
IF Frequency	60 MHz
IF Bandwidth	15 MHz
Front End	Waveguide (WR-28)

Figure 2 is a photograph of the radar system including the Scientific Atlanta tracking pedestal all mounted on a specifically designed trailer for ease of portability. Mobility is a key feature of this millimeter wave radar system. The radar moves from site to site on the trailer and remains on the trailer during testing. A set of side racks are mounted around the perimeter of the trailer which together with overhead hoops and canvas tarpaulins provide a removable protective shelter for the radar. This shelter provides adequate protection from the weather and environment, but does not sacrifice portability of the overall system. The assembled shelter on the trailer is shown in Figure 3. Figure 4 is a photograph of the radar instrumentation and control consoles which are transported from site to site by truck.

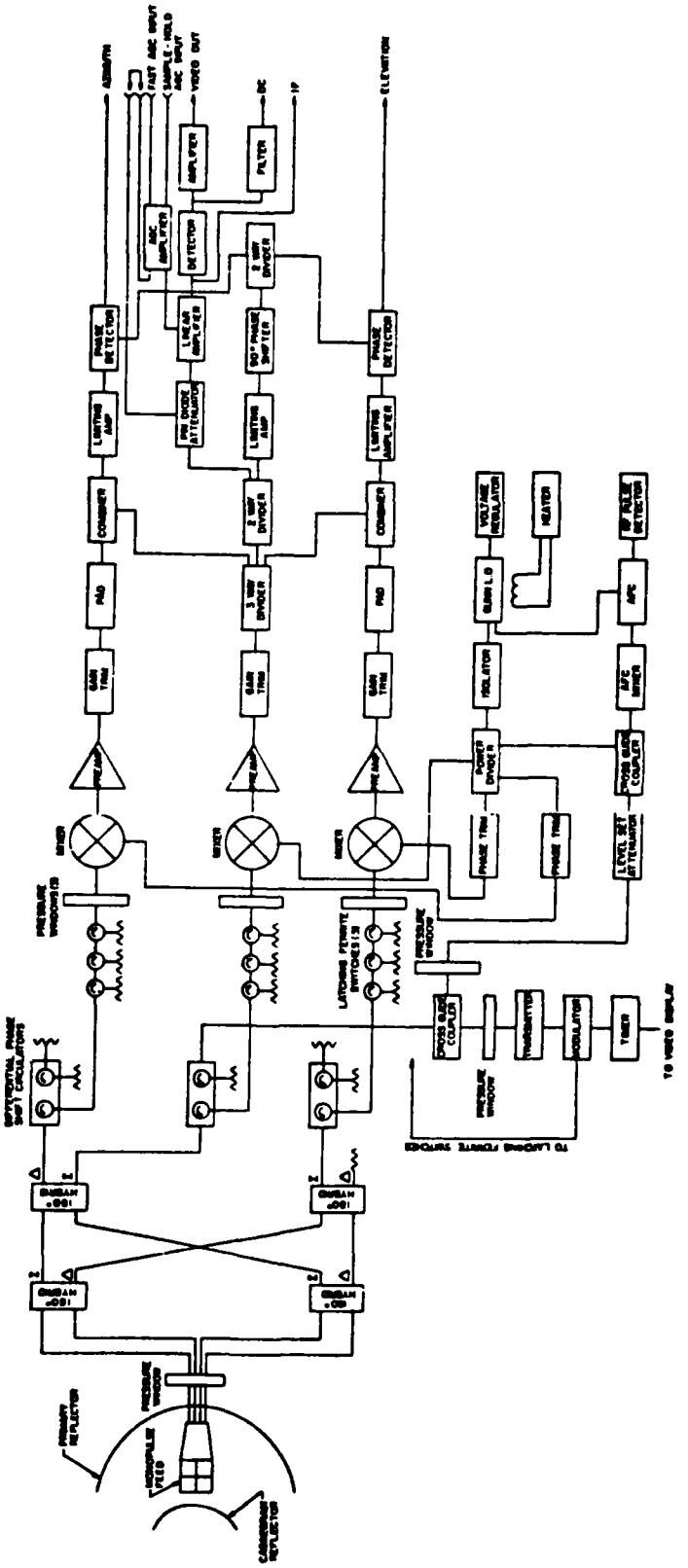

Figure 1. Radar Front End Block Diagram

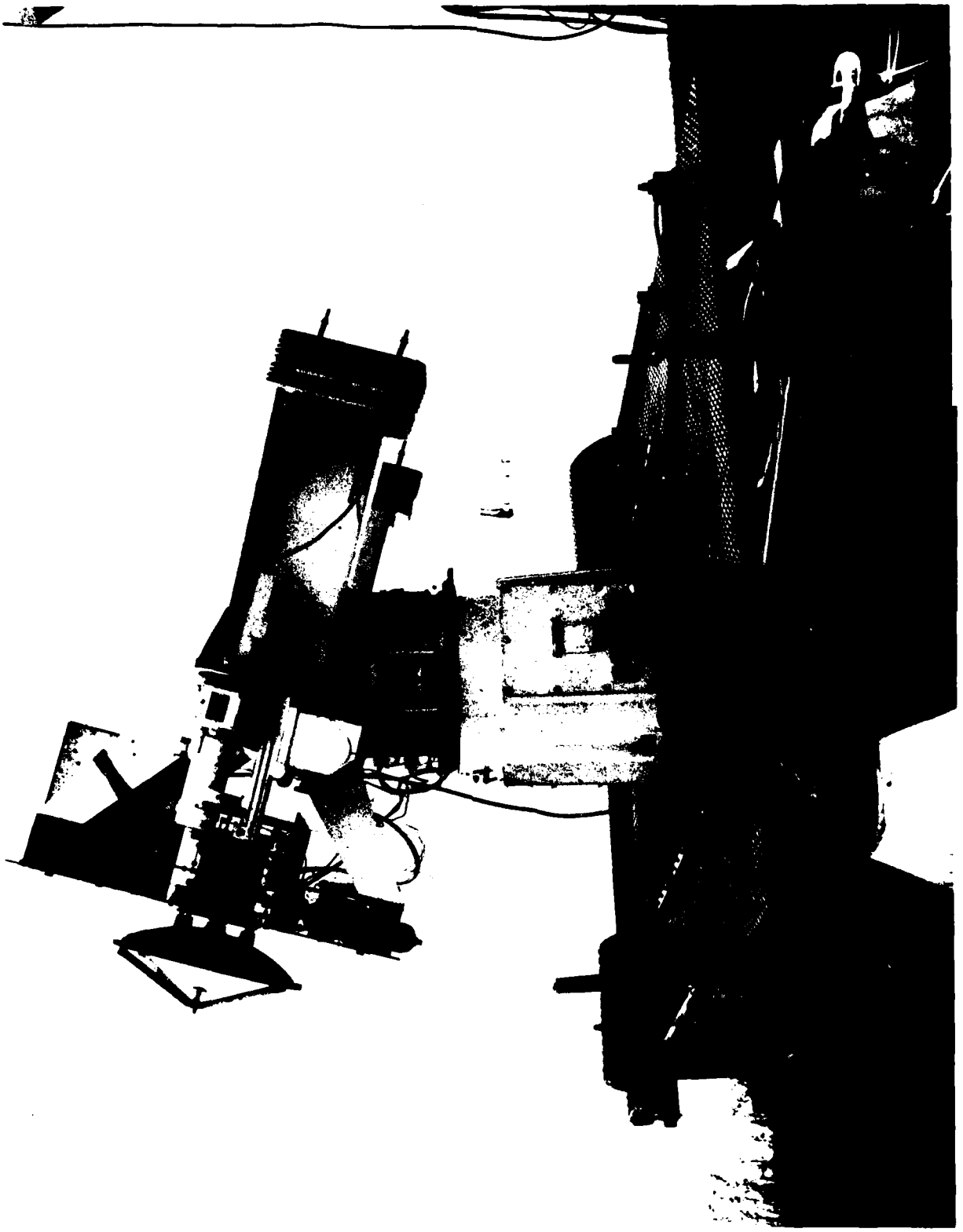

Figure 2. Radar System on Trailer

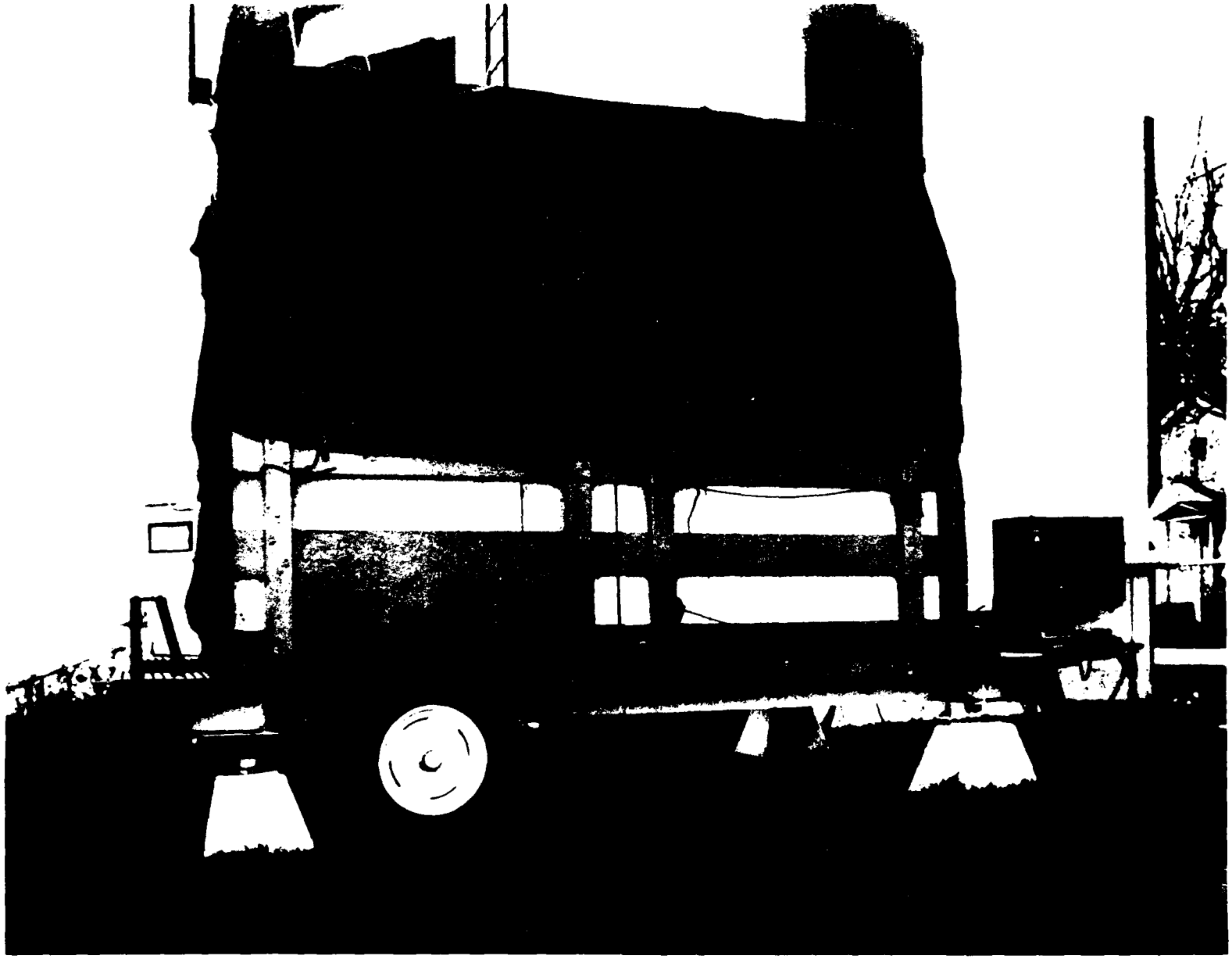

Figure 3. Radar System with Shelter Assembled on Trailer

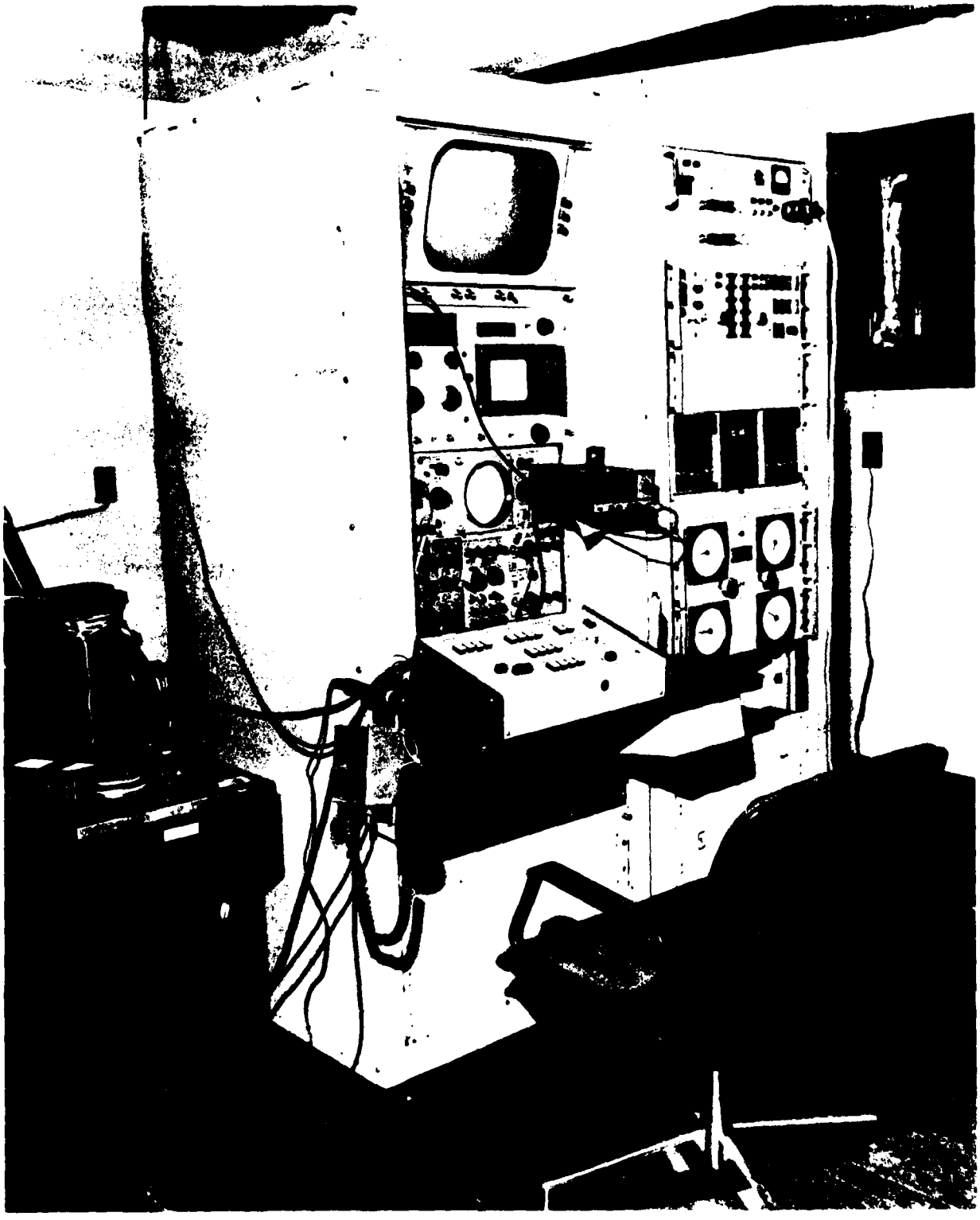

Figure 4. Radar Control and Display Console

ANTENNA AND COMPARATOR

The antenna is of the Cassegrain type and consists of a 2-ft diameter paraboloid reflector, a smaller hyperboloid reflector, and a four-horn monopulse feed. Polarization of the antenna is linear vertical with capability built in to change to horizontal or circular. Peak gain of the sum channel is 43 dBi with a 1° beamwidth. The sum channel side lobes are -18 dB nominal and the difference channel side lobes are -16 dB. These side lobe levels are both with respect to the sum channel peak. The null depth of the difference pattern is -35 dB with respect to the sum pattern peak. The insertion loss of the monopulse comparator is 0.75 dB nominal in any one channel. The comparator contains phase shifters to equalize the electrical length of all three channels. Power handling capability is 100 kW peak and 55 W average when pressurized to 8 psi with sulfahexafluoride (SF_6) gas. Figure 5 is a graph of the peak pulse power handling capability of WR-28 waveguide as a function of pressurization.

The antenna plus the monopulse comparator network is an amplitude comparison system capable of providing azimuth and elevation sum and difference patterns for tracking in the two planes. The sum channel has a maximum amplitude level for a radar target return signal centered in the main beam (arriving along the boresight axis). The difference channel has a minimum output for a target centered in its radiation pattern along the boresight axis of the antenna (see Figure 6). The antenna characteristics and the radio frequency (RF) monopulse comparator network shape the RF signal envelope in the difference channel such that this minimum signal level defines the lowest point of a deep, sharp null. This null characteristic of the difference channel allows the monopulse radar to measure the angle to the target very precisely.

The amplitude sensing antenna system has four closely spaced feed horns that produce four radiation patterns that are displaced from the antenna boresight axis. This displacement is termed beam squint and is a function of the separation of the feed horn phase centers from the focal point of the antenna aperture. Each of the four radiation patterns are identical, and do not completely overlap each other. They intersect on the boresight axis of the antenna. All radar signals arriving within the beamwidth of the antenna, except those on the boresight axis will be unequal by an amount proportional to the angle off the boresight axis. The two signals in each plane (Az and El) are then subtracted in the monopulse comparator to produce a difference signal also proportional to the angle off the boresight axis, since the radiation patterns have equal amplitudes on this axis. A sense is also provided due to the subtraction process in the difference channel to discriminate left from right in azimuth or up from down in elevation. The monopulse comparator consists of four folded "T" hybrids to form the sum channel, azimuth difference channel, and elevation difference channel. The signals from the four antenna feeds are input to the four hybrids as shown in the simplified block diagram of Figure 7. The hybrid sum arm and the hybrid difference arm are used to obtain the sum and difference signal respectively.

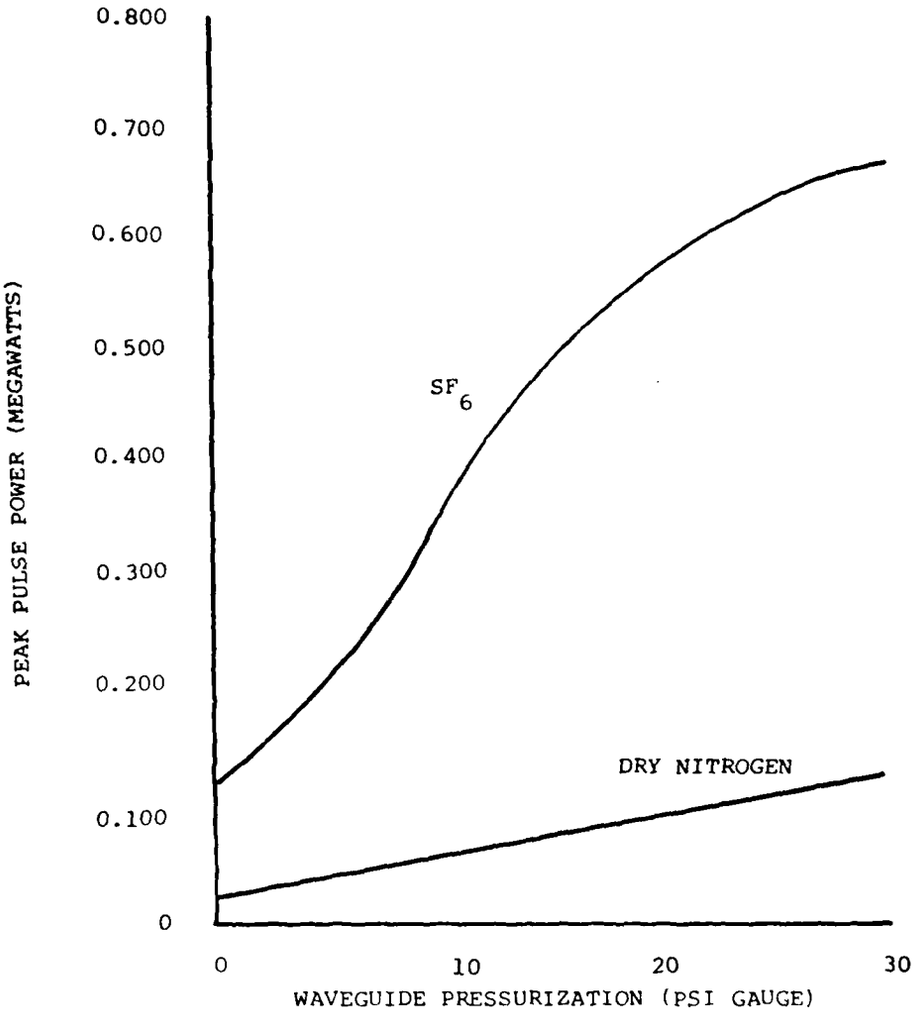

WR-28 waveguide (26-40 GHz)

Factor of Safety = 2

68°F Temperature

VSWR $\leq$ 1.5:1

Figure 5. Peak Pulse Power Handling Capability of WR-28 Waveguide as a Function of Pressurization

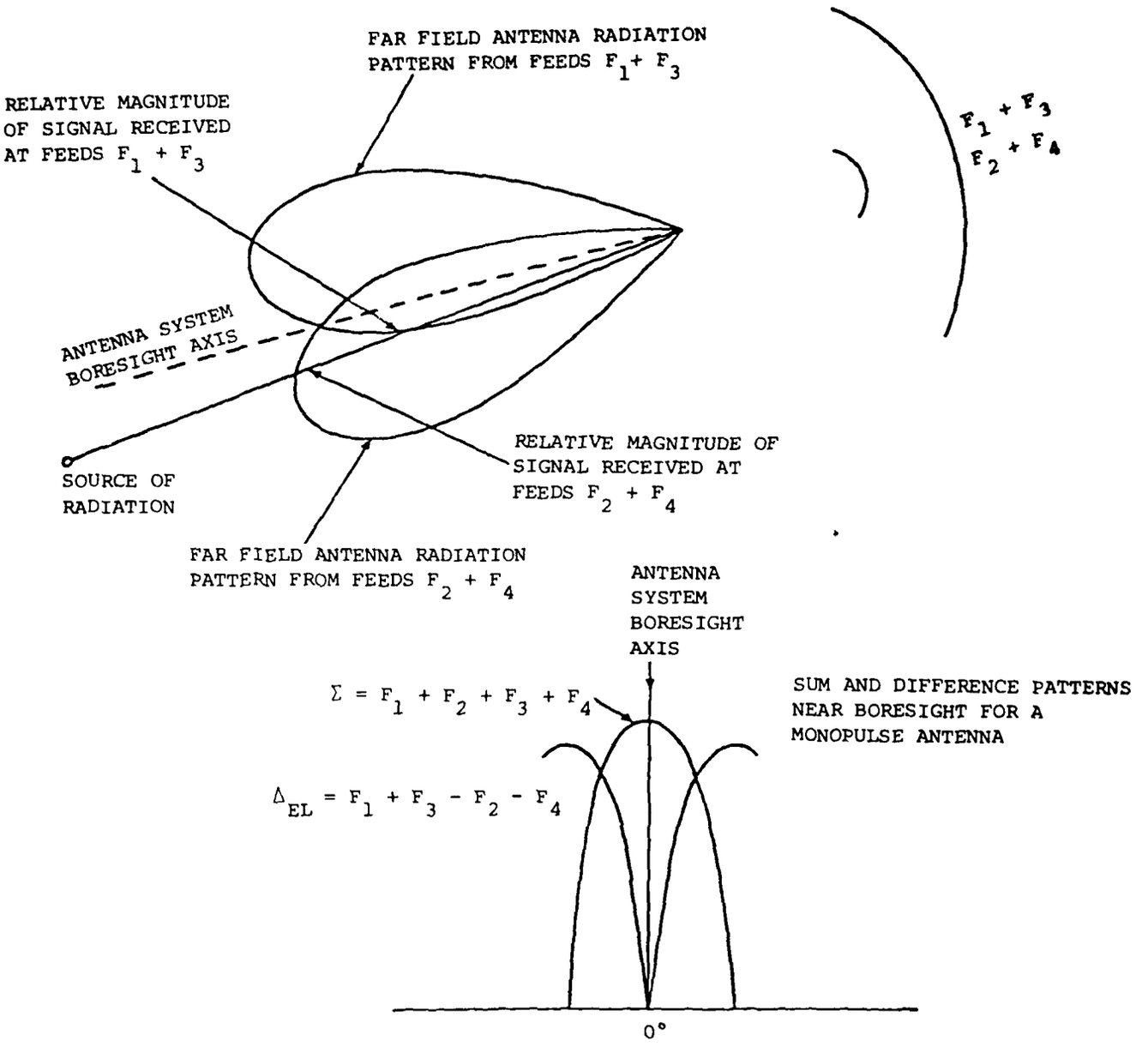

Figure 6. Amplitude Sensing Antenna Patterns and the Relative Magnitude of Signals Received by Each Feed

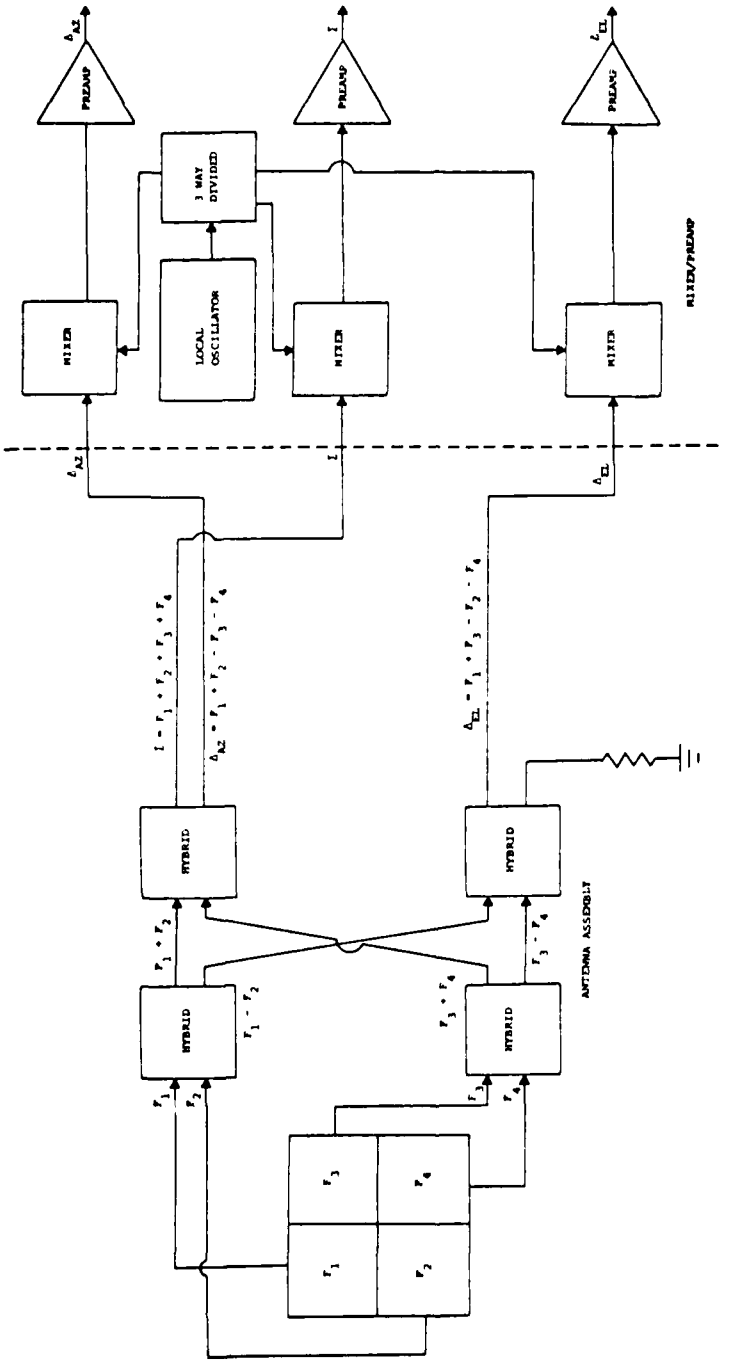

Figure 7. Simplified Antenna and Receiver Block Diagram

TRANSMITTER

The transmitter module (see Figure 8) contains the 35-GHz magnetron and the complete modulator electronics. A separate control panel for operating the transmitter is contained in the instrument control rack for convenience of radar operation during tests. The transmitter tube is a Varian SFD-319, inverted coaxial magnetron capable of over 100 kW peak and 55 W average power (0.00055 maximum duty factor). This tube differs from the conventional magnetron in that the geometry of the cathode and anode is interchanged (see Figure 9). In a conventional magnetron the anode surrounds the cathode. For millimeter wave frequencies this severely limits the maximum physical size of the cathode, because the size of this element is comparable to a wavelength. The smaller the cathode the shorter the life of the tube. In an inverted coaxial magnetron tube the cavity is located inside a slotted cylinder with a resonator vane array arranged around the outside. The cathode is then formed as a ring around the anode. The end result is that the cathode current densities are reduced to one-tenth of that used in the conventional (cathode-centered) magnetron. This design technique makes a long life magnetron practical at millimeter wavelengths. Coupling out of the cavity is in the circular waveguide mode which has a very low transmission loss.

The solid state modulator can modulate the tube with three pulsewidths (0.1, 0.5, 1.0 μsec) and has selectable pulse repetition frequencies (PRFs) of 275-5500 pps. The modulator is a hybrid solid state magnetic modulator. The critical switching is performed by a magnetic device. For high power and narrow pulses it is necessary to go to magnetic devices in a modulator. The high power dictates high voltage magnetic devices and the narrow pulses require the pulse fidelity obtainable from magnetic devices. The entire transmitter weighs 125 lb. A power reduction network (see Figure 10) permits reduction of transmitter output power delivered to the antenna by 10, 20, 30, or 40 dB. An additional coupler provides transmitter RF information to the automatic frequency control (AFC) mixer. The transmitter output reduction waveguide, antenna, and receiver up to but not including the latching ferrite circulators are all pressurized to 8 psi with SF_6.

DUPLEXER

The duplexer (see Figure 11) consists of three latching ferrite switches and one differential phase shift circulator per channel. The differential phase shift circulators are unnecessary in the difference channels for circuit protection, but they provide better channel-to-channel dynamic phase tracking. A synchronizer triggers the latching ferrites into the high attenuation state just prior to the main bang of the transmitter. An interlock prevents the transmitter modulator from being triggered until the latching ferrites are in this high attenuation state. A loss of waveguide pressurization will also prevent the

Figure 8. Radar Transmitter

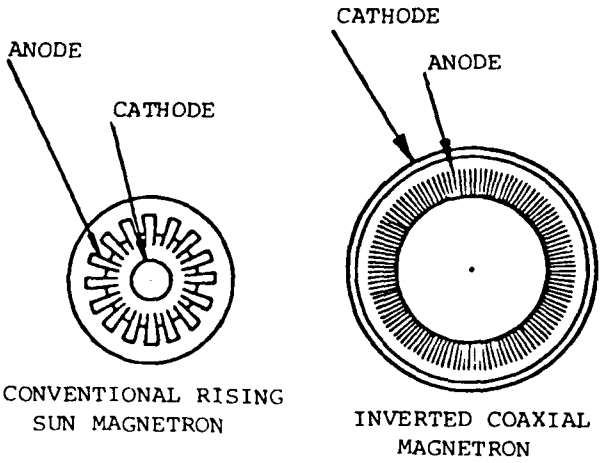

Figure 9. Comparison of a Conventional Rising Sun Magnetron with an Inverted Coaxial Magnetron Designed to Operate at the Same Frequency

transmitter from being triggered. A current transformer in the magnetron tube circuit senses the main bang of the transmitter and switches the latching ferrites to their low attenuation state after a short delay. The total isolation between the transmitter and receiver is 80 dB during the transmit pulse. The trigger circuitry is fed by transistor transistor logic (TTL) signals. A trigger circuit converts this TTL trigger pulse to a 28-V pulse, and then triggers the three separate triple stage latching ferrite sections of the receiver. (Each of the three receiver protection circulators consists of three latching ferrite circulators in series.) Inside each device is additional circuitry for triggering each section simultaneously. The leading edge of the trigger pulse is processed by the trigger circuitry into a positive high current spike that creates a high magnetic field which latches the ferrite material into the high attenuation state. The trailing edge of the same pulse is converted to a negative high current spike that reverses the direction of the magnetic field in the ferrite material causing it to go to the low attenuation state. Turn-on and turn-off time for the latching ferrite material is illustrated in Figure 12.

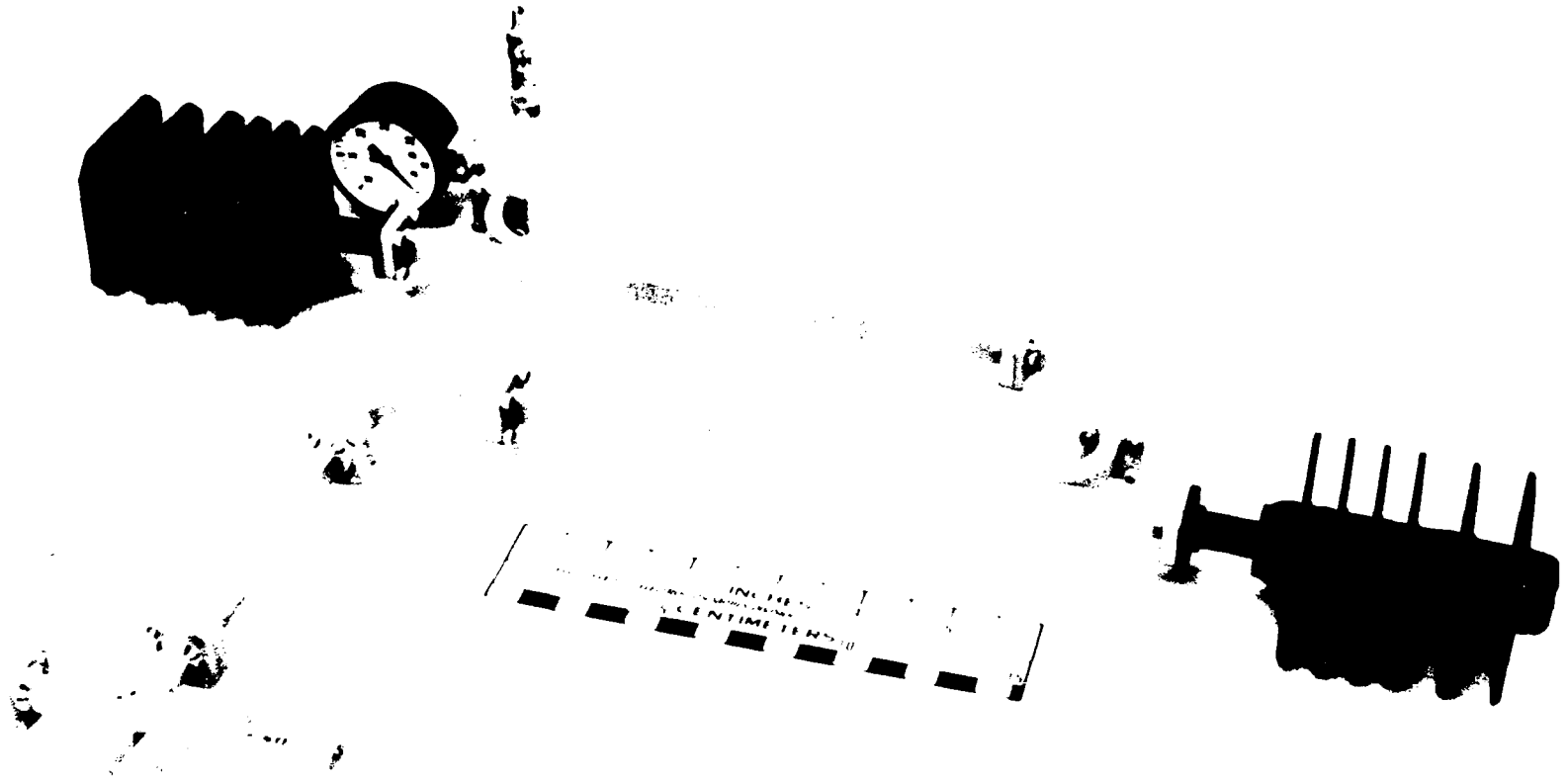

Figure 10. Transmitter Power Reduction Network

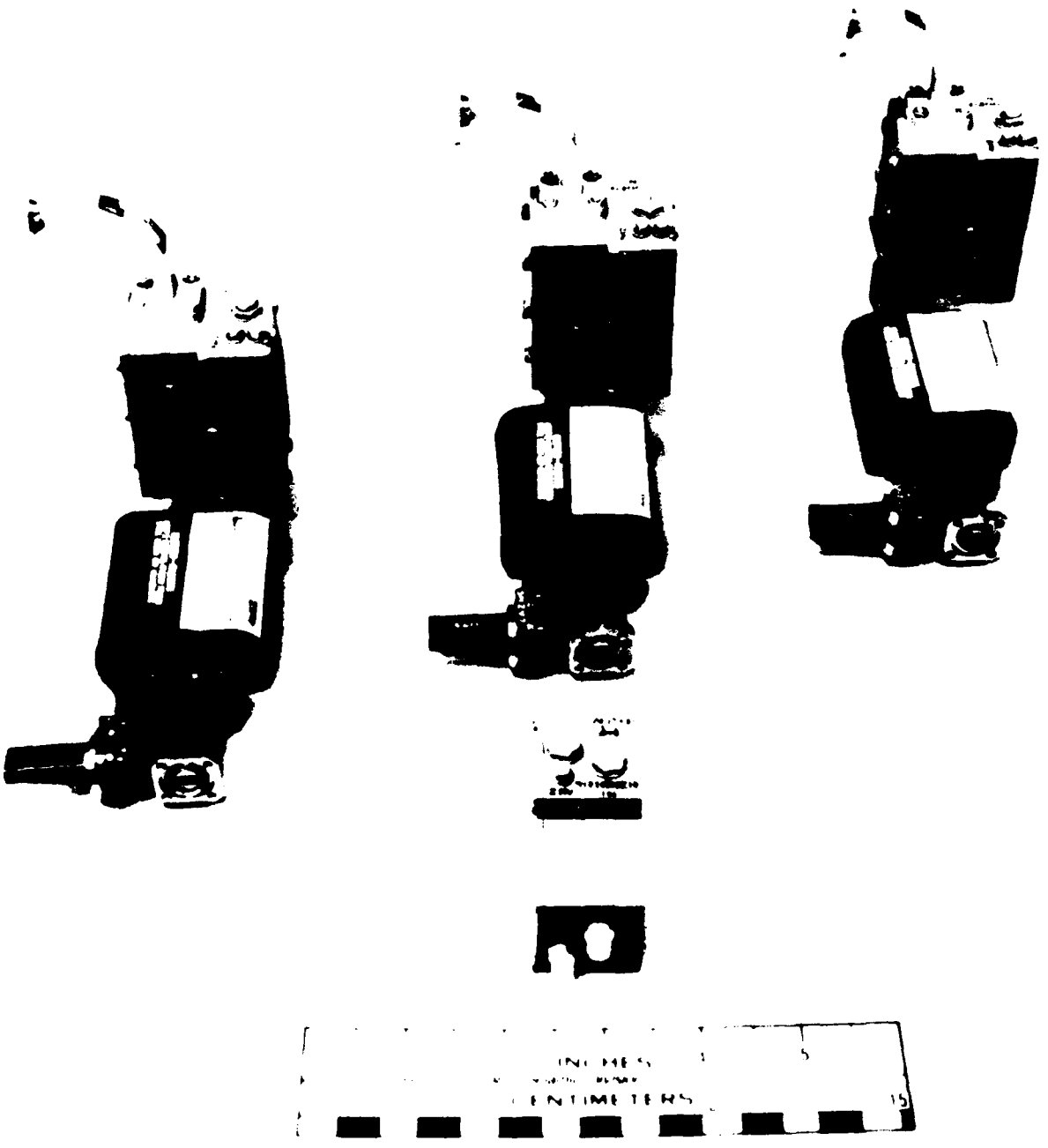

Figure 11. Millimeter Wave Radar Duplexer

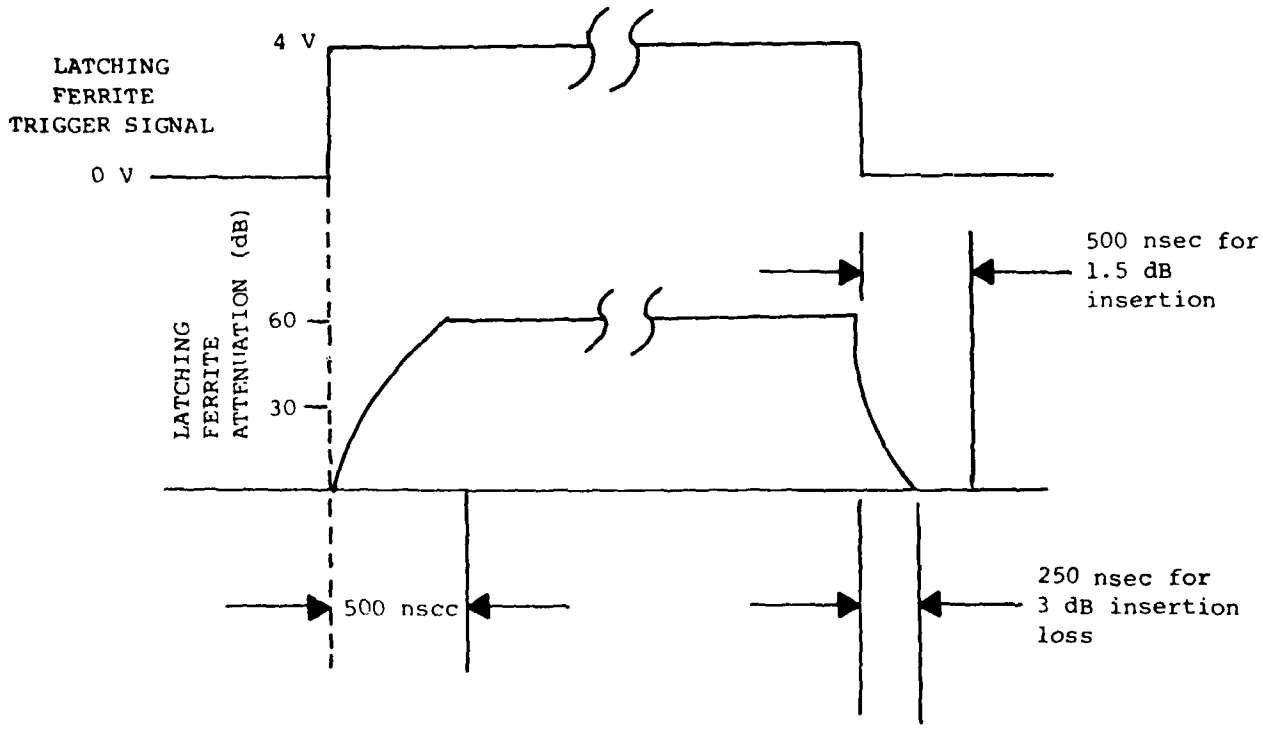

Figure 12. Latching Ferrite Turn-On and Turn-Off Times

MONOPULSE RF RECEIVER

The three-channel monopulse receiver (see Figure 13) has four low noise balanced mixer/preamp modules (5-dB DSB noise figure); one for each of the three receiver channels (sum, azimuth difference, elevation difference) and one for the AFC channel. Each mixer (see Figure 14) contains two silicon Schottky Barrier diodes. The mixer preamps have a 1-dB compression point of -10 dBm. The total RF/intermediate frequency (IF) gain of the mixer/preamp combination is 32 dB. There is a 3-dB loss in each receiver channel prior to the mixer which results in a -39 dBm maximum input level for linear operation. This 3-dB loss is the combined insertion losses of the input waveguide, pressure windows, latching circulators, and monopulse comparator. The dynamic range of the receiver is therefore -91 to -39 dBm. The overall receiver noise figure is 8 dB DSB.

The local oscillator is a 170-mW varactor tuned Gunn diode oscillator. The frequency can be tuned over a 100-MHz bandwidth using a 0 to -9 V tuning range provided by the AFC discriminator circuit. The AFC consists of a Travis type frequency modulation discriminator followed by a pulse integrator, dc error amplifier and a voltage controlled oscillator driver for tuning the varactor diode. The AFC determines the difference between the local oscillator and transmitter frequencies via the AFC mixer/discriminator and compares this to 60 MHz. If the frequency is different than 60 MHz, the AFC closed loop circuit provides the appropriate correction voltage to tune the local oscillator such that a 60-MHz difference is achieved.

Referring to the system block diagram of Figure 1, there is a phase trimmer in each of the difference channel local oscillator legs to adjust the IF phase of the down-converted difference channels with respect to the sum channels. The required phase difference for IF signal processing is 90°, so that the sum and difference signals can be added in phase quadrature and converted from amplitude to phase information. This is covered in more detail in the IF section description. Pin diode attenuators (see Figure 1) provide gain trim in all three receiver channels.

MONOPULSE IF PROCESSING

The monopulse intermediate frequency (MIF) amplifier subsystem (see Figure 15) of the receiver accepts the three outputs from the sum, azimuth difference, and elevation difference channel mixer/preamps and converts the amplitude/phase information into phase only information. Referring to the block diagram of Figure 16, the two difference channels are then converted by the video processor to provide steering commands for the tracking pedestal. The sum channel is first split into three channels; two of these channels are combined with the difference channels for angle processing, the third channel is then split two ways to provide a phase reference for the angle channel phase comparators, and a sum channel

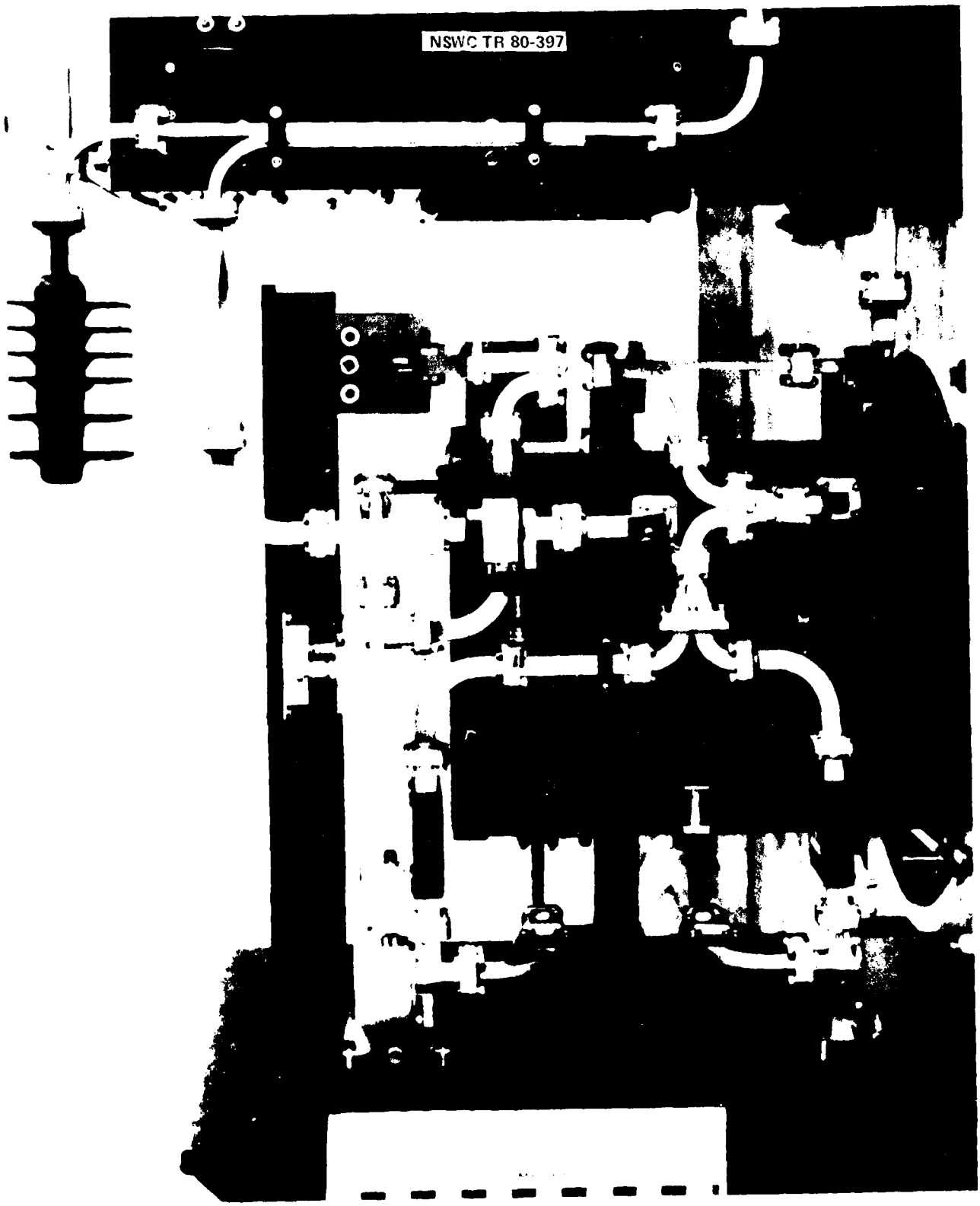

Figure 13. Millimeter Wave Radar Receiver

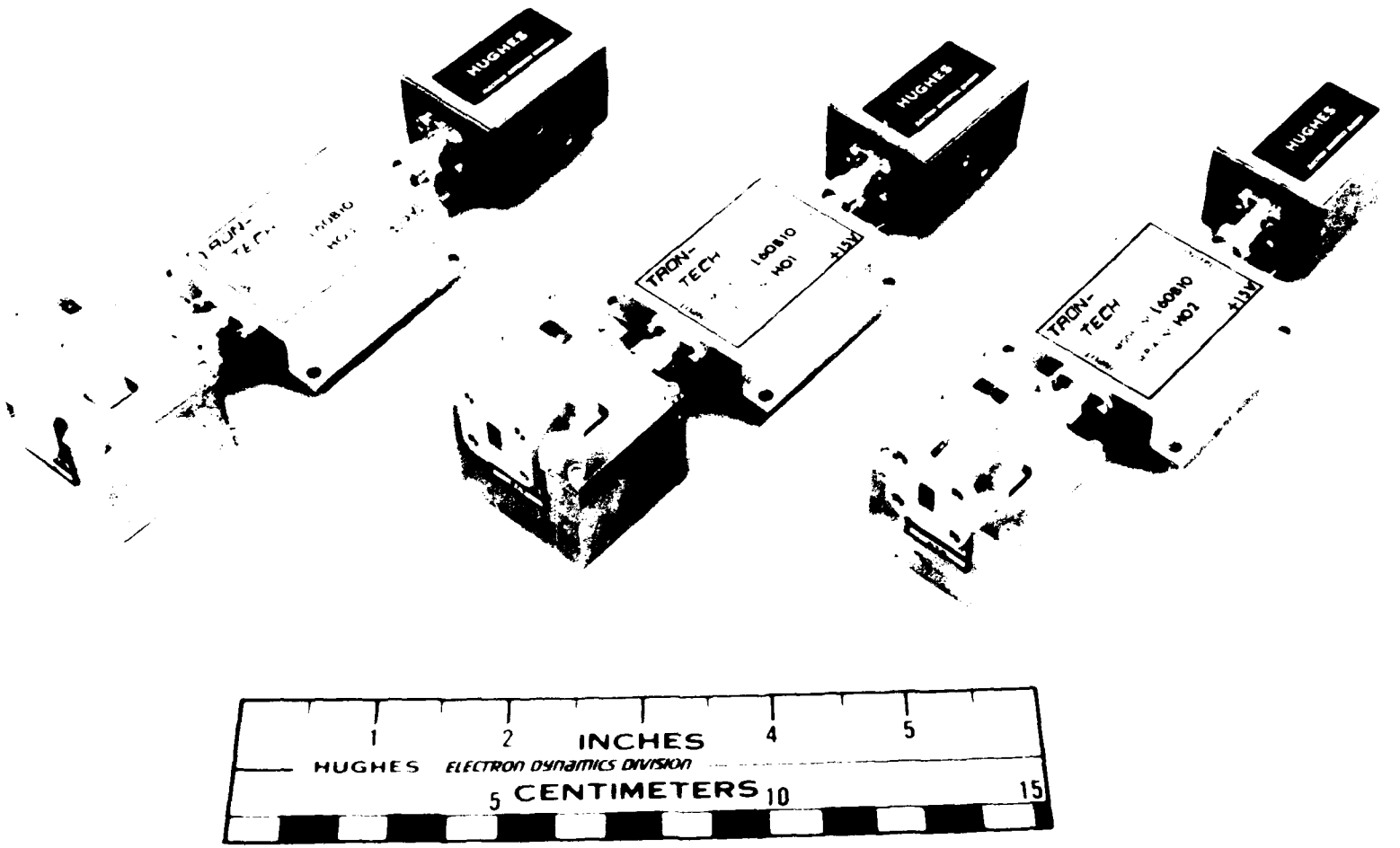

Figure 14. Silicon Schottky Barrier Diode Balanced Millimeter Wave Mixer

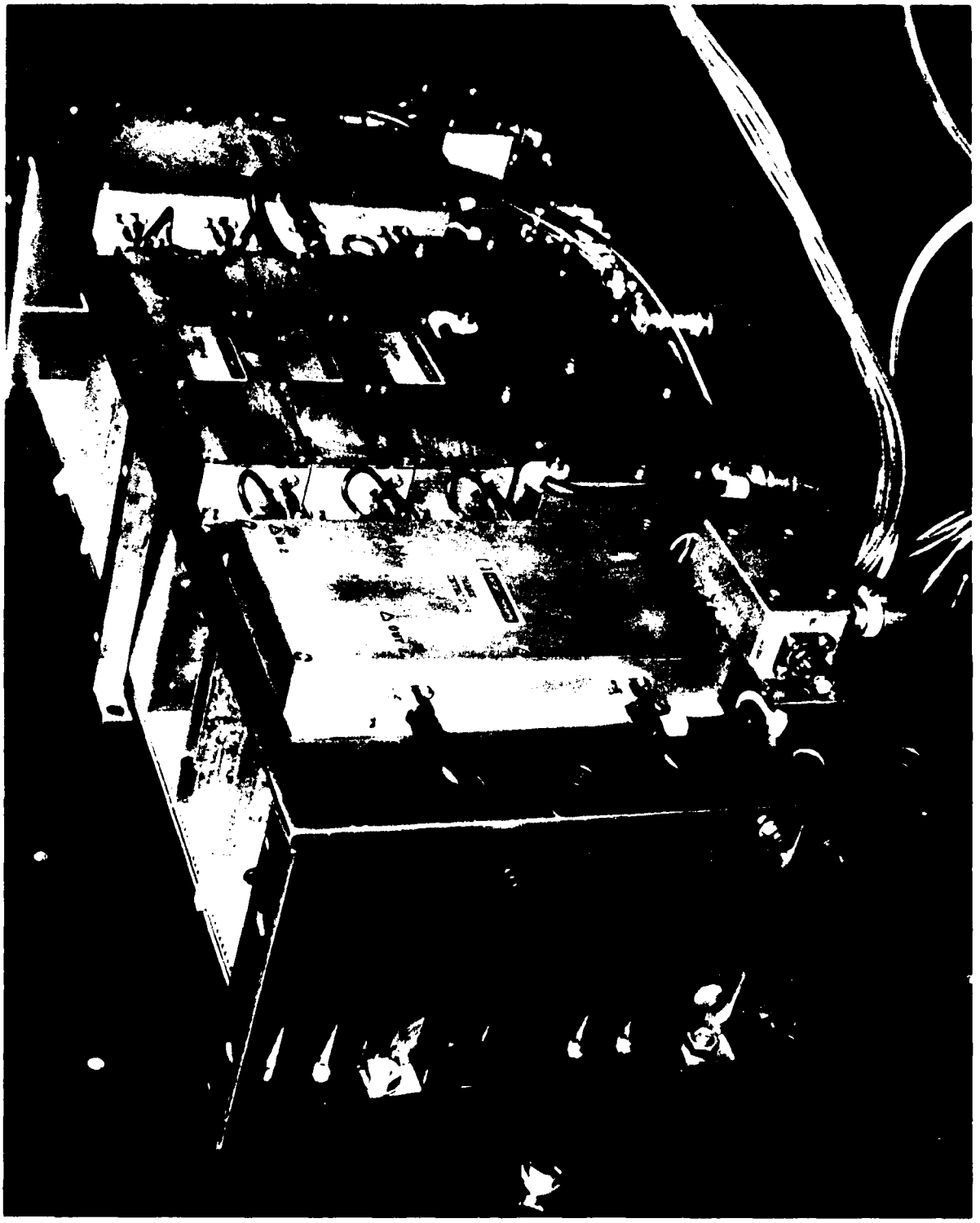

Figure 15. Radar Receiver IF Assembly

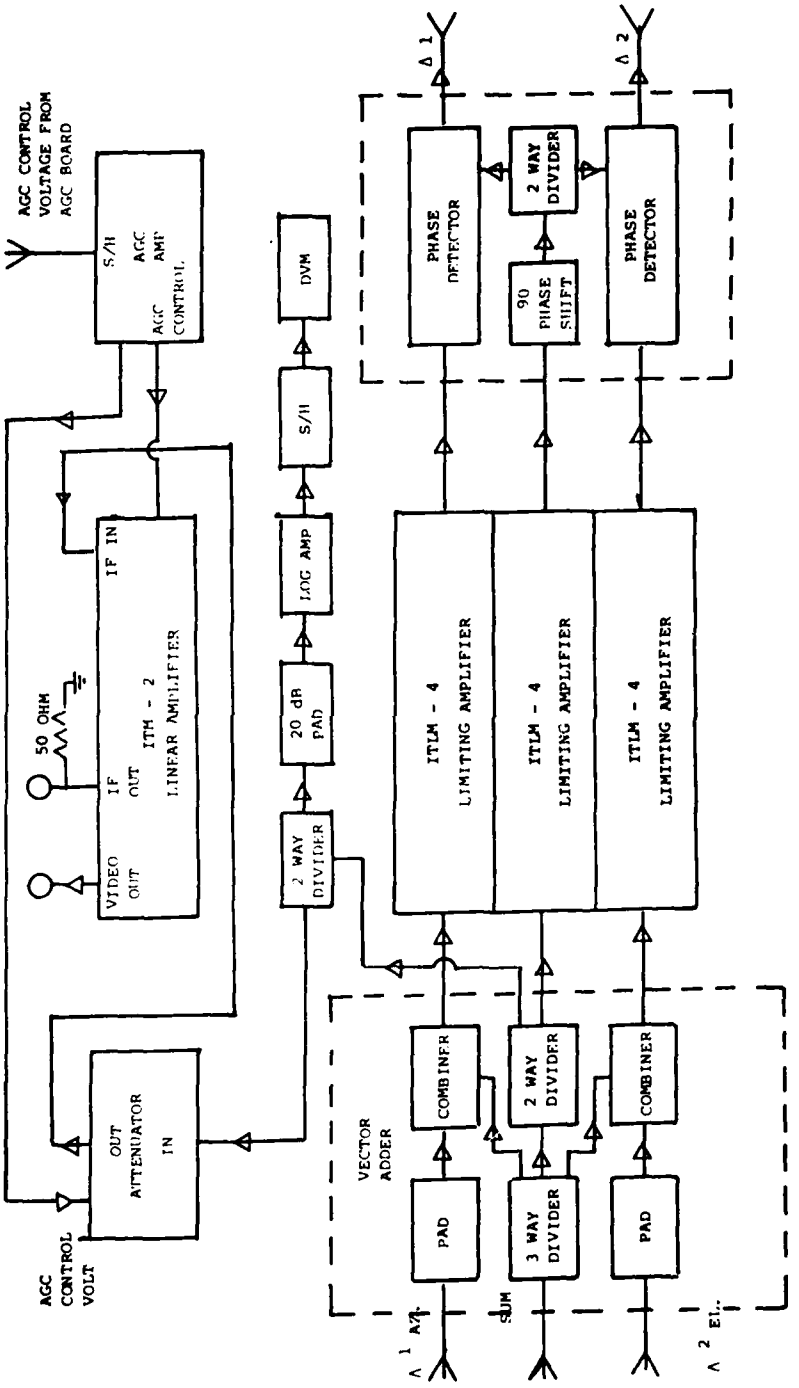

Figure 16. MIF Block Diagram

for the IF/video acquisition circuit. The phase reference is inputted to a limiting amplifier and delayed by 90° to provide a reference for both angle channel phase comparators. The two sum channels from the first power split are vector added with the difference channels in a signal combiner. Since the difference channel signals are in phase quadrature with the sum signal, the amplitude information is converted to phase information by vector addition. The output of the combiner is a signal whose phase is proportional to the angle off the boresight axis. The output of each combiner is then inputted to a limiting amplifier whose output still contains the phase information, but no amplitude variations. The phase of each of the difference channels is compared to the delayed sum channel in two phase detectors. The output of each phase detector is proportional to $\cos(\theta-90°)$ where $(\theta-90°)$ is the phase difference between the two phase detector input signals, and θ is proportional to the angle of the target off the boresight axis. The phase information is thus converted to amplitude information. The phase tracking between the sum (Σ) and each sum plus difference ($\Sigma + J\Delta$) limiting amplifier channel is typically less than 2°, since the difference in signal levels between each channel is very small. The three MIF outputs are then fed to a video signal processor for conversion to dc error signals to provide steering information for tracking the target and the appropriate output voltages for range gate tracking and display purposes.

VIDEO PROCESSOR

The video processor (see Figure 17) consists of circuitry that performs the following functions: acquisition, range tracking, angle processing, synchronizer, automatic gain control (AGC) processing, display processing, and AFC discrimination. The video processor also contains the log IF amplifier and its sample/hold circuit for conversion of the log IF output pulse to a dc level representing received signal power. Each of these subsystems incorporates recent technological advances in integrated circuit and solid state devices technology to attain high performance levels while simultaneously reducing the system size and complexity thus retaining high reliability and serviceability.

RADAR CONTROL AND DISPLAY CONSOLE

The radar control and display console (see Figure 4) contains all the necessary equipment for remotely controlling the radar, display circuitry for observing system performance, and recording instrumentation for collecting data during the tests. Displays provided include an A-scope, a B-scope, a TV picture of the target scene, a digital range display, and a received signal power indicator. The A-scope provides signal amplitude versus range plus a range tracking symbol. The B-scope provides azimuth angle and range information using signal amplitude for display intensity when the radar is used in the sector scan mode. An additional display on the B-scope panel is the digital range readout. The A-scope display

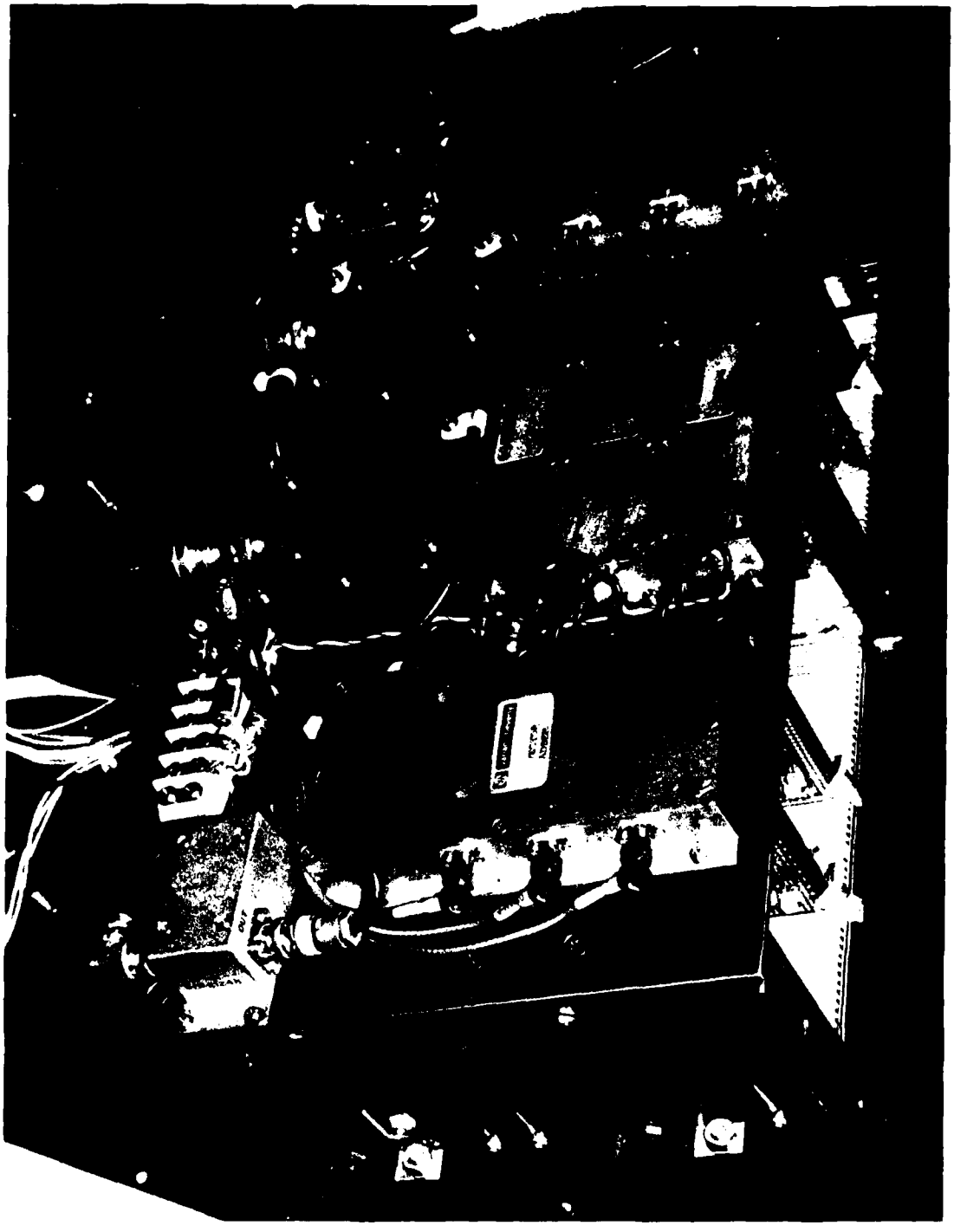

Figure 17. Video Processor (Sheet 1 of 2)

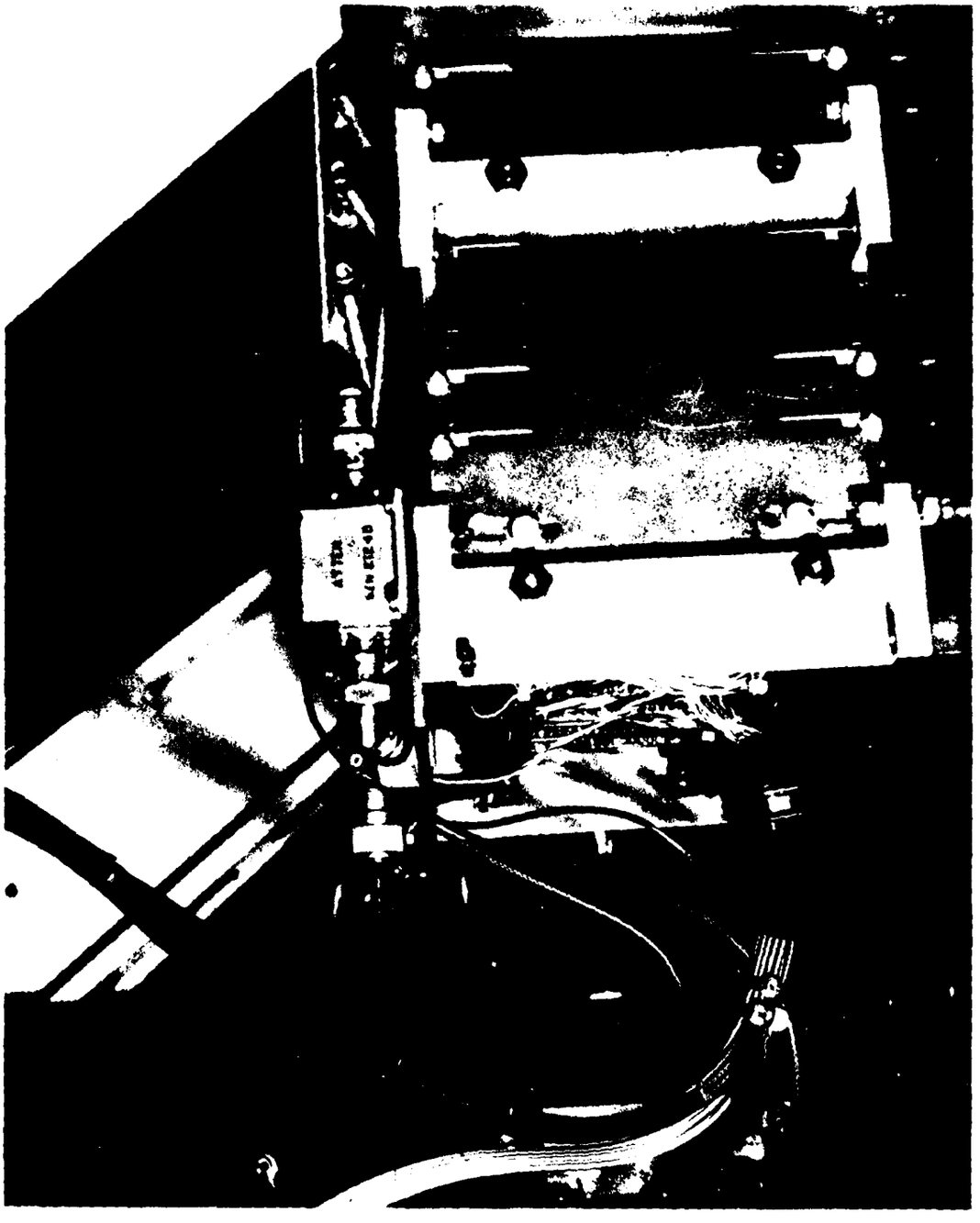

Figure 17. Video Processor (Sheet 2 of 2)

and the logarithmic amplifier output voltmeter are monitored with a TV camera whose video output is multiplexed into a split-screen format on the target scene video camera output and recorded on a video recorder. The primary data acquisition system is a video recorder. A TV monitor provides a visual image display of the target scene. The TV camera that displays the target scene is boresighted to the radar and contains both wide angle and telephoto lenses.

A split screen TV capability displays the range readout, received signal and A-scope simultaneously with the target scene. An electronically generated tracking symbol superimposed on the TV monitor target scene provides an instantaneous indication of where the monopulse radar sees the target. The azimuth and elevation coordinates of this track symbol are directly controlled by the unfiltered radar azimuth and elevation error signals. The track symbol has a much faster time constant than that of the tracking pedestal and therefore can follow the instantaneous radar steering errors more accurately than the pedestal.

Acquisition of targets is performed manually using the boresighted TV camera and a joystick pedestal control. The target is manually positioned in the center of the TV screen via the joystick. An automatic range acquisition and track is then initiated by the operator. An operator controlled switch then connects the radar steering commands to the pedestal servo control channels to initiate angle tracking.

TRACKING PEDESTAL

The entire radar, which weighs about 400 lb, is mounted in a Scientific Atlanta 3100 series tracking pedestal. This unit is capable of slew rates of up to 30°/sec and slew accelerations of $30°/(sec)^2$. It can travel ±370° in azimuth and -5 to +185° in elevation. A sector scan device automatically scans the pedestal ±20° in azimuth and +20 to -5° in elevation. The pedestal weight is 800 lb. Input power required is 208/120 V, 60 Hz, three phase, four wire. The static error and power gearing backlash are both 0.05°.

RADAR SYSTEM PERFORMANCE ANALYSIS

RADAR SYSTEM PERFORMANCE ANALYSIS SYNOPSIS

A system analysis was conducted to provide predictions on what level of performance could be obtained with the millimeter wave radar after it was built. This analysis provided the necessary information for carrying out the test program and assisted in identifying any problem areas to be encountered in the

application of millimeter wave techniques to Navy radars. The following areas were investigated:

1. Prediction of maximum detection range performance using a computer implemented Blake model in a clear environment, clutter, environment, and in the presence of multipath.

2. Predictions of signal level as a function of range due to clutter and multipath interference.

3. Monopulse angle and range tracking accuracies as a function of thermal noise, multipath, target glint, target motion, and the servomechanism induced errors of the tracking pedestal.

4. The low angle tracking problem.

5. Performance in an ECM environment.

DETECTION RANGE CALCULATIONS

The detection ranges for the monopulse radar were calculated using several methods. One method calculates the detection range of the radar in "quasi-free" space. The calculated range is based on the assumption of free-space wave propagation modified only by the effects of the normal atmosphere, including molecular absorption losses and normal refraction, but not including absorption by rain or other precipitation, abnormal refractive effects, or multipath interferences. The refractive losses are the lens effect loss, and absorption losses are those due to oxygen and water vapor absorption. The detection range was calculated for this method using the standard radar parameters of Figure 18 and the statistics of detection criteria, Pd = 0.9 and $P_{fa} = 1(10^{-6})$. An additional required input is the target size and its fluctuation characteristics. The results for a one-square meter nonfluctuating target and a one-square meter Swerling Case 1 are presented in Table 2.

A second detection range calculation method includes the additional effects of multipath and the vertical plane radiation pattern of the radar antenna. The output is in the form of a range-height-angle profile of the vertical plane radar coverage. Figure 19 is an example of this vertical plane radar coverage for the first parameter combination of Figure 18.

The third detection range calculation provides a plot of the return signal versus range for a target approaching the radar at constant altitude. This method also takes into account sea-reflection, multipath, interference, and is the only one of the three methods that includes the effects of clutter. This

Pulse Power, kW	100.0
Pulse Length, μsec	See Table Below
PRF, Hz	See Table Below
Bandwidth Correction Factor, C_B, dB	See Table Below
Number of Pulses Integrated, n	See Table Below
Duty Cycle	.00055
Transmit Antenna Gain, dB	43.0
Receive Antenna Gain, dB	43.0
Frequency, MHz	35,000
Receiver Noise Figure, dB	8.0
Antenna Ohmic Loss, dB	1.5
Transmit Transmission Line Loss, dB	1.5
Receive Transmission Line Loss, dB	3.0
Scanning Antenna Pattern Loss, dB	1.6
Horizontal Beamwidth, degrees	1.0
Vertical Beamwidth, degrees	1.0
Side Lobe Level, dB	18.0
Antenna Polarization	Vertical

PRF (Hz)	Pulsewidth (μsec)	Number of Pulses (n)	C_B (dB)
5.5×10^3	0.1	110	+2.03
1.1×10^3	0.5	23	+3.29
$.55 \times 10^3$	1.0	11	+6.03

Figure 18. Millimeter Wave Radar System Parameters

Table 2. Detection Range Performance in Clear Air

Code Number	Antenna Tilt Angle (deg)	Target Angle (deg)	Nonfluctuating One-Square Meter Target: Detection Range (nmi)	Tropo Loss (dB)	S/N* (dB)	Swerling Case 1 for One-Square Meter Target: Detection Range (nmi)	Tropo Loss (dB)	S/N* (dB)
1	0	~0	13.8	5.26	-1.5	9.2	3.57	7.0
2	0	~0	14.8	5.91	2.76	10.2	4.10	11.1
3	0	~0	13.5	6.14	4.97	9.3	4.27	13.2
1	0.5	0.5	13.9	5.14	-1.5	9.3	3.49	7.0
2	0.5	0.5	14.9	5.73	2.76	10.3	4.01	11.1
3	0.5	0.5	13.6	5.96	4.97	9.3	4.17	13.2
1	1.0	1.0	14.0	4.96	-1.5	9.4	3.43	7.0
2	1.0	1.0	15.1	5.55	2.76	10.2	3.89	11.1
3	1.0	1.0	13.8	5.75	4.97	9.4	4.06	13.2
1	3.0	3.0	14.6	4.38	-1.5	9.6	3.13	7.0
2	3.0	3.0	15.9	4.83	2.76	10.6	3.52	11.1
3	3.0	3.0	14.5	4.96	4.96	9.6	3.65	13.2

Code Number	Pulsewidth (μsec) PRF (Hz) Number of Pulses (N)
	0.1
1	5.5×10^3
	110
	0.5
2	1.1×10^3
	23
	1.0
3	$.55 \times 10^3$
	11

* S/N = Required signal to noise ratio

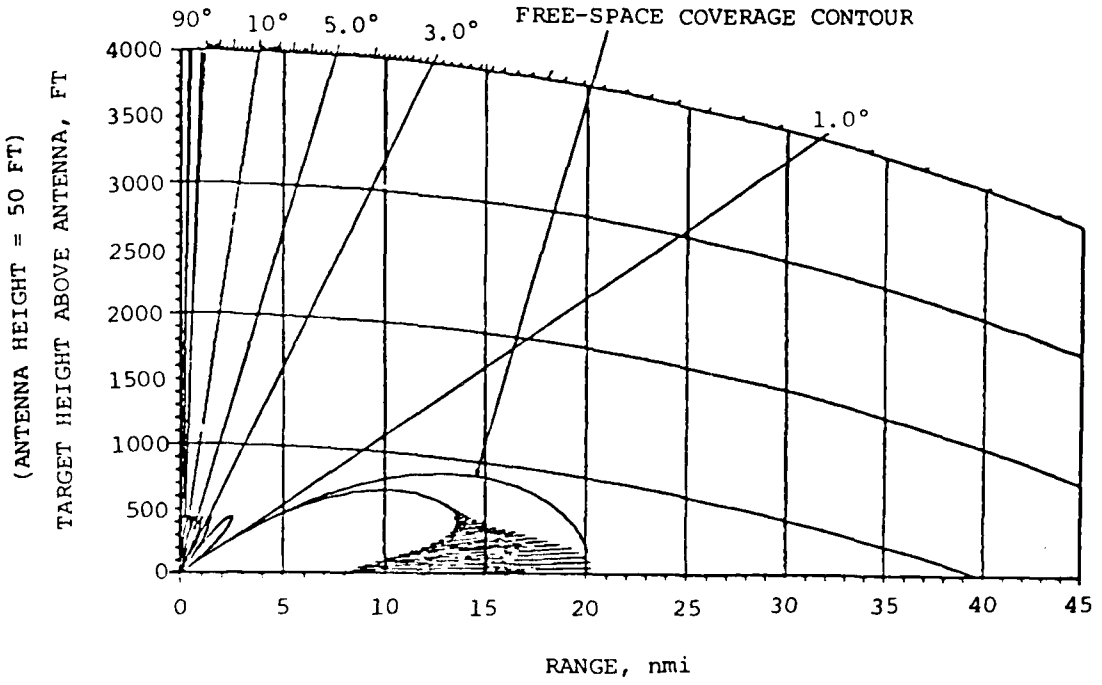

Figure 19. Lobe Plot

technique is particularly suited for the case of a low altitude target for which the information contained from the second method vertical plane coverage is inadequate. When the plotted signal is above a certain threshold, as indicated on the graph by different lines or curves for different conditions, the target is detectable.

The threshold is determined by the minimum detectable signal, clutter and any ECM environment. A sample performance curve is included in Figure 20.

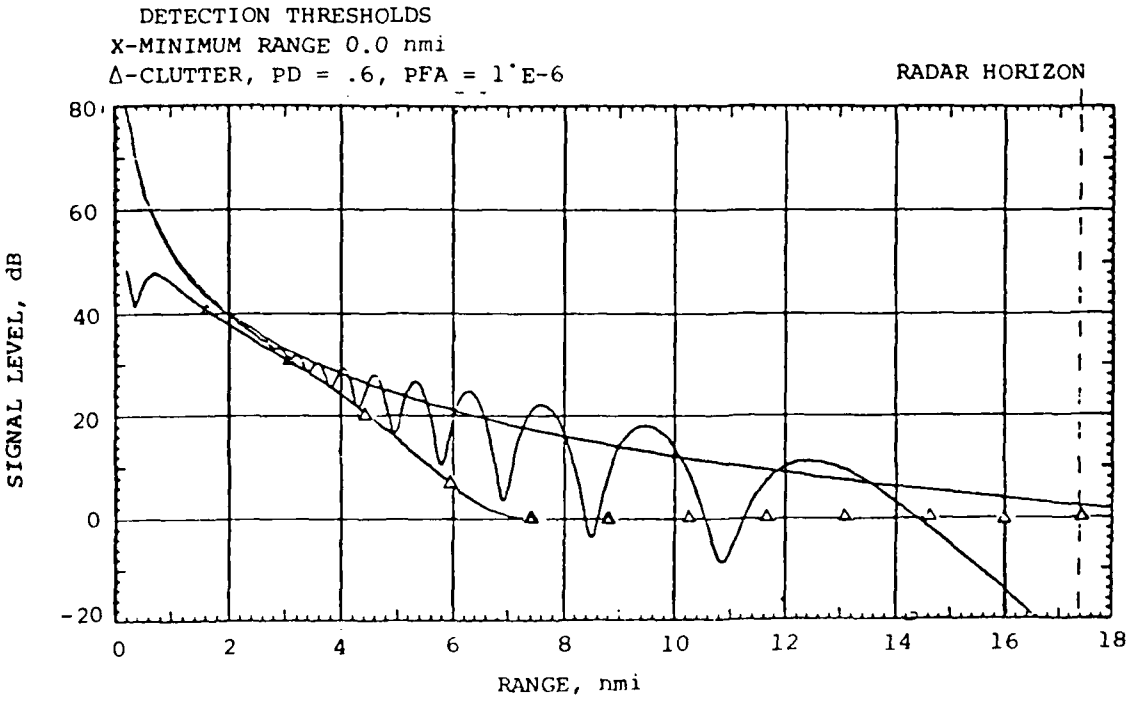

Figure 20. Signal Level vs Range

ANGLE TRACKING ACCURACY

The angle tracking accuracies of the millimeter wave radar were calculated using the measured system parameters of the actual hardware. These tracking accuracies are a function of many independent variables: signal to noise ratio (S/N), multipath, target glint, monopulse network imbalances, clutter, atmospheric refraction, and the error characteristics of the tracking pedestal servomechanism. Each of these variables becomes more or less significant depending on target height, speed and heading relative to the radar. For example, a high altitude target at short range would have a negligible multipath and clutter induced error. A high speed crossing target would have a larger dynamic lag error than a stationary target. The effects of each variable were computed for each of the cases listed in Table 3. The total errors for each combination of situations were calculated by summing the squares of each error contributed by all of the variables and then taking the square root of the result. The total error is listed in Table 3 for each case.

The thermal angle tracking error as a function of S/N was computed and is shown plotted in Figure 21. This error is also directly proportional to antenna beamwidth.

The root-mean-square value (RMS) Multipath Angle Tracking Error as a function of target elevation angle is shown in Figure 22. The maximum error is shown at 0.33° and occurs when the lower difference channel elevation main lobe peak is coincident with the surface of the water directly below the target at the same range. The error curve follows the antenna difference pattern in shape, but the target elevation angle is exactly half that of the antenna difference pattern, because of the target and surface geometry with respect to the radar (see Figure 23).

Target glint or the apparent wander of the point of track on and about the target is dependent on the reflection characteristics and geometric extent of the target.

The monopulse network errors are caused by phase and amplitude imbalances in the antenna, RF receiver, and signal processing. These errors were balanced out in the system as part of the radar calibration exercise. The effects of these imbalances are to cause boresight angle error shifts and angle channel sensitivity changes. This topic is treated in detail in reference 1.

The clutter effects are a function of signal to clutter ratio and the antenna parameters. They do not represent the effects of multipath which were treated previously.

Atmospheric refraction error effects are negligible at the short ranges under consideration.

The tracking pedestal servomechanism errors include the effects of: power gearing backlash, static error, orthogonality, wind loading, and dynamic lag to provide an estimate of all errors induced by the tracking pedestal.

Table 3. RMS Radar Angle Tracking Errors

	Total Error (mrad)	Total Error Minus Servo Errors (mrad)
Point Target at Low Angle $\theta_{elev} = .35°$	Az .42 El 2.13	Az .11 El 2.10
Point Target at High Angle $\theta_{elev} > 1.0°$	Az .42 El .37	Az .11 El .11
Distributed Target at Low Angle $\theta_{elev} = .35°$	Az 2.33 El 2.21	Az 2.30 El 2.19
Distributed Target at High Angle $\theta_{elev} > 1.0°$	Az 2.34 El .70	Az 2.30 El .61
Crossing Point Target at Low Angle $\theta_{elev} > 1.0°$ $V_t = 500$ mph	Az .66 El 2.13	Az .11 El 2.10
Crossing Point Target at High Angle $\theta_{elev} > 1.0°$ $V_t = 500$ mph	Az .66 El .37	Az .11 El .11
Crossing Distributed Target at Low Angle $\theta_{elev} = .35°$ $V_t = 500$ mph	Az 1.65 El 2.27	Az 1.52 El 2.24
Crossing Distributed Target at High Angle $\theta_{elev} > 1°$ $V_t = 500$ mph	Az 1.65 El .86	Az 1.52 El .78

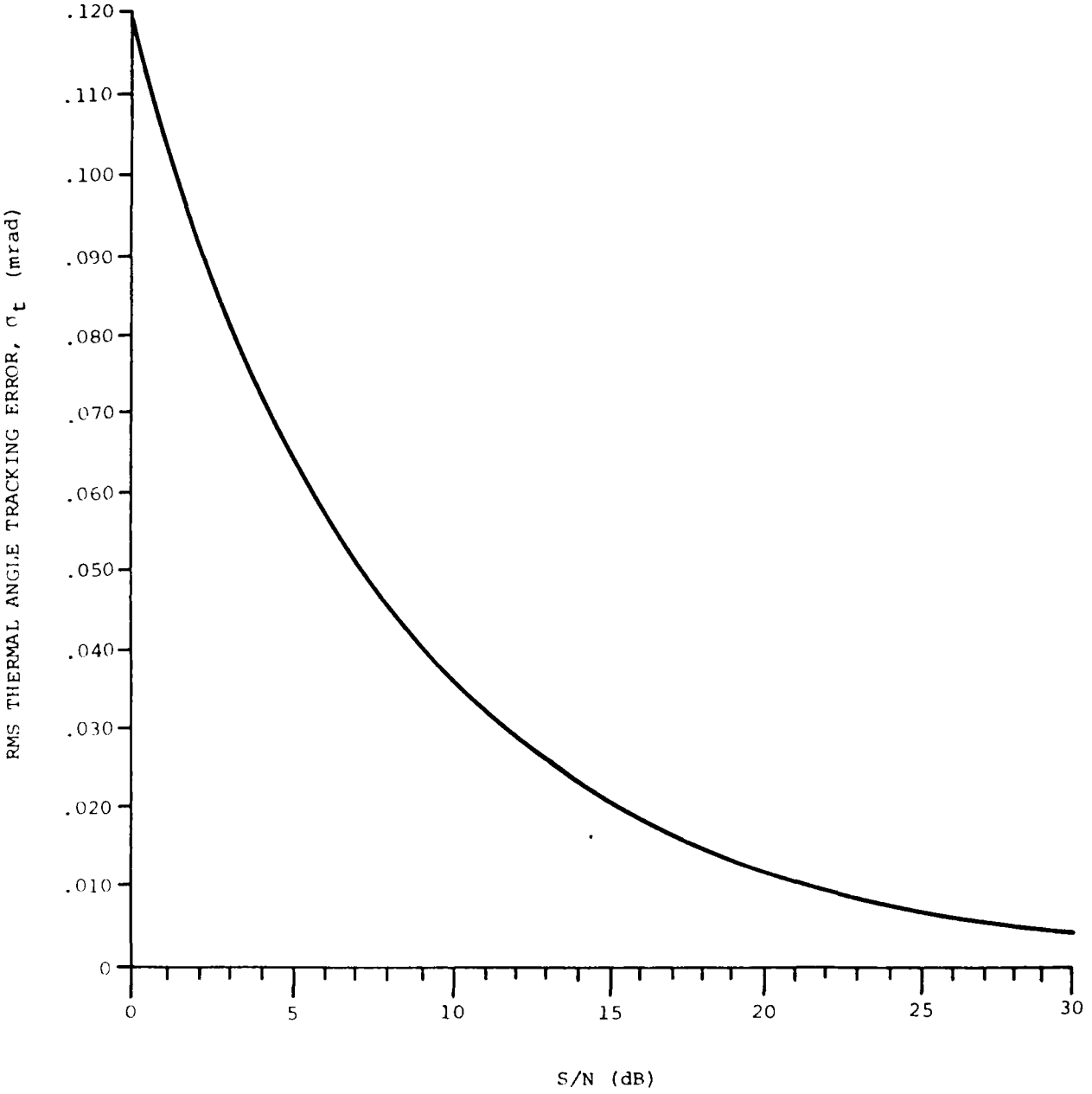

Figure 21. Thermal Angle Tracking Error vs S/N

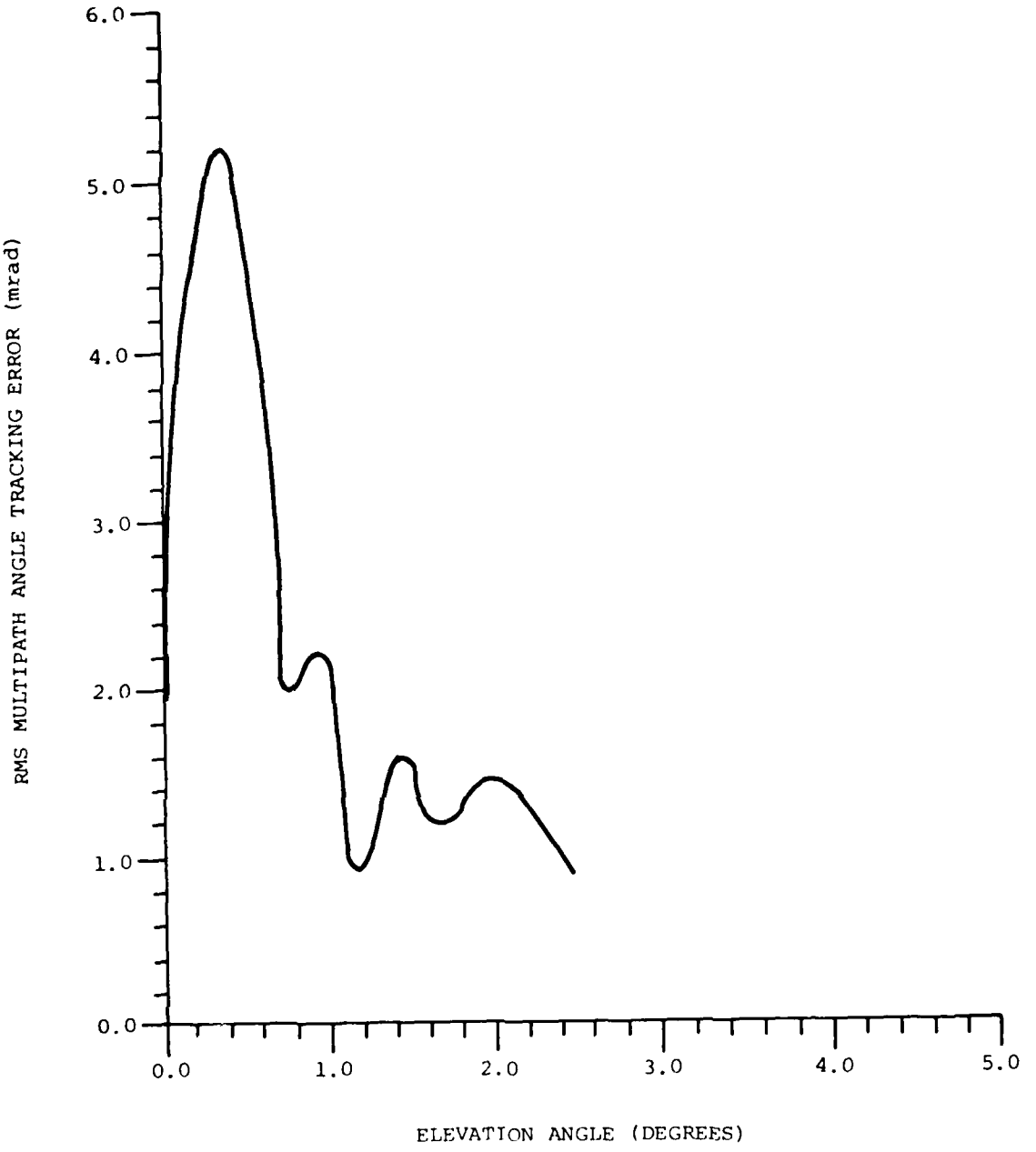

Figure 22. Multipath Angle Tracking Error vs Target Elevation Angle

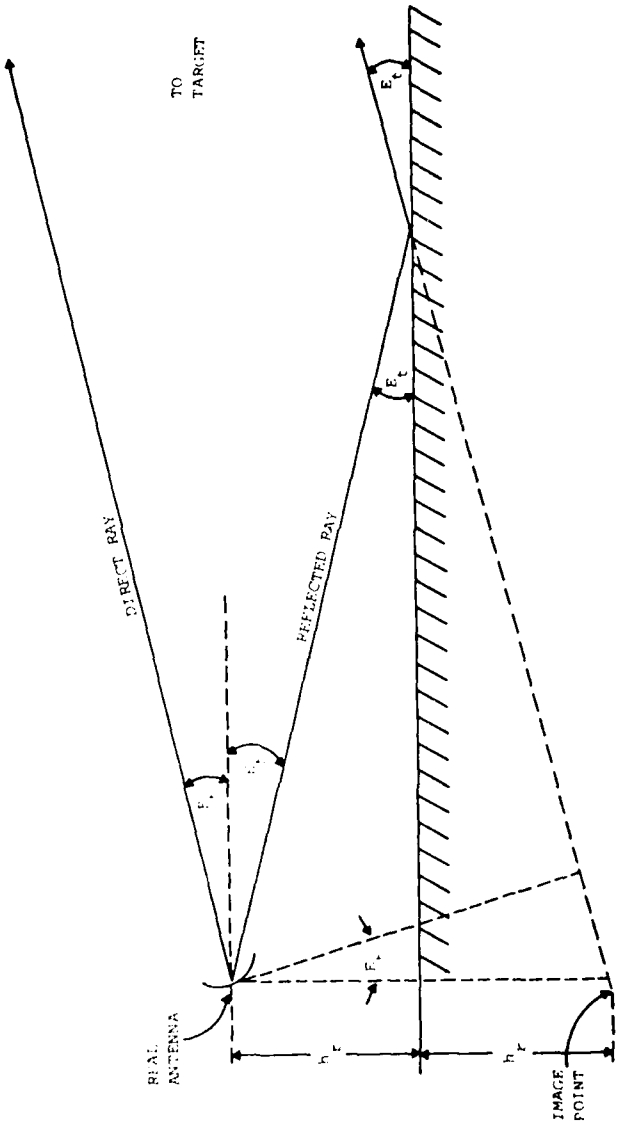

Figure 23. Radar Target and Surface Geometry for Multipath Conditions

RANGE TRACKING ACCURACY

The range tracking accuracy was calculated using the actual measured system parameters of the millimeter wave radar. Radar range tracking accuracy is dependent on the thermal noise environment, range multipath noise and bias, and the errors induced by the range measuring electronics. The thermal range tracking error due to noise is plotted vs S/N for three pulsewidths in Figures 24, 25, and 26.

The range multipath noise and bias is dependent on target elevation angle and the radar antenna pattern. These errors are plotted in Figure 27. The total range multipath error is the RMS range multipath error variation added directly to the bias error.

The range error contributed by the electronics in the range discriminator varies from approximately ±10 ns peak at 0.5 nmi to ±50 ns peak at 15 nmi. These time errors translate into distance errors of ±5 ft and ±25 ft peak respectively. The total range tracking error is obtained by taking the square root of the sum of the squares of each error contribution. Table 4 contains selected cases for the total error.

LOW ANGLE TRACKING PROBLEM

The detection and tracking of targets at very low elevation angles with conventional radars at the low microwave frequencies has always been a problem because of the inability of the radar to resolve the image target from the real target. This inability is a direct result of the wide radar antenna pattern elevation beamwidth and the specular nature of reflection from an irregular surface (the sea) at microwave frequencies. The following discussion will attempt to clarify the problem and demonstrate how a millimeter wave radar achieves improved low angle tracking.

Figure 28 defines the angles and distances for the radar and target geometries used in the discussion. Also shown are the definition of points of specular reflection and areas of diffuse scattering. These points of specular reflection (smooth surface) and areas of diffuse scattering (rough surface) were calculated for different target heights and radar ranges. The results are presented in Table 5. This information is useful in predictions of radar performance and allows a better evaluation of the test site geometry.

For a smooth surface the reflection is termed specular and is a point on the surface representing the point of reflection for multipath interference. The angle of the location of this point with respect to the radar antenna boresight is important, because it can be used to determine the transmitted power level of the reflection by means of the antenna patterns. The power level incident in the receiver can also be determined from the antenna patterns and the angle of reflection. For low angle tracking the radar will attempt to track this image point of the target if the reflected signal level is sufficient.

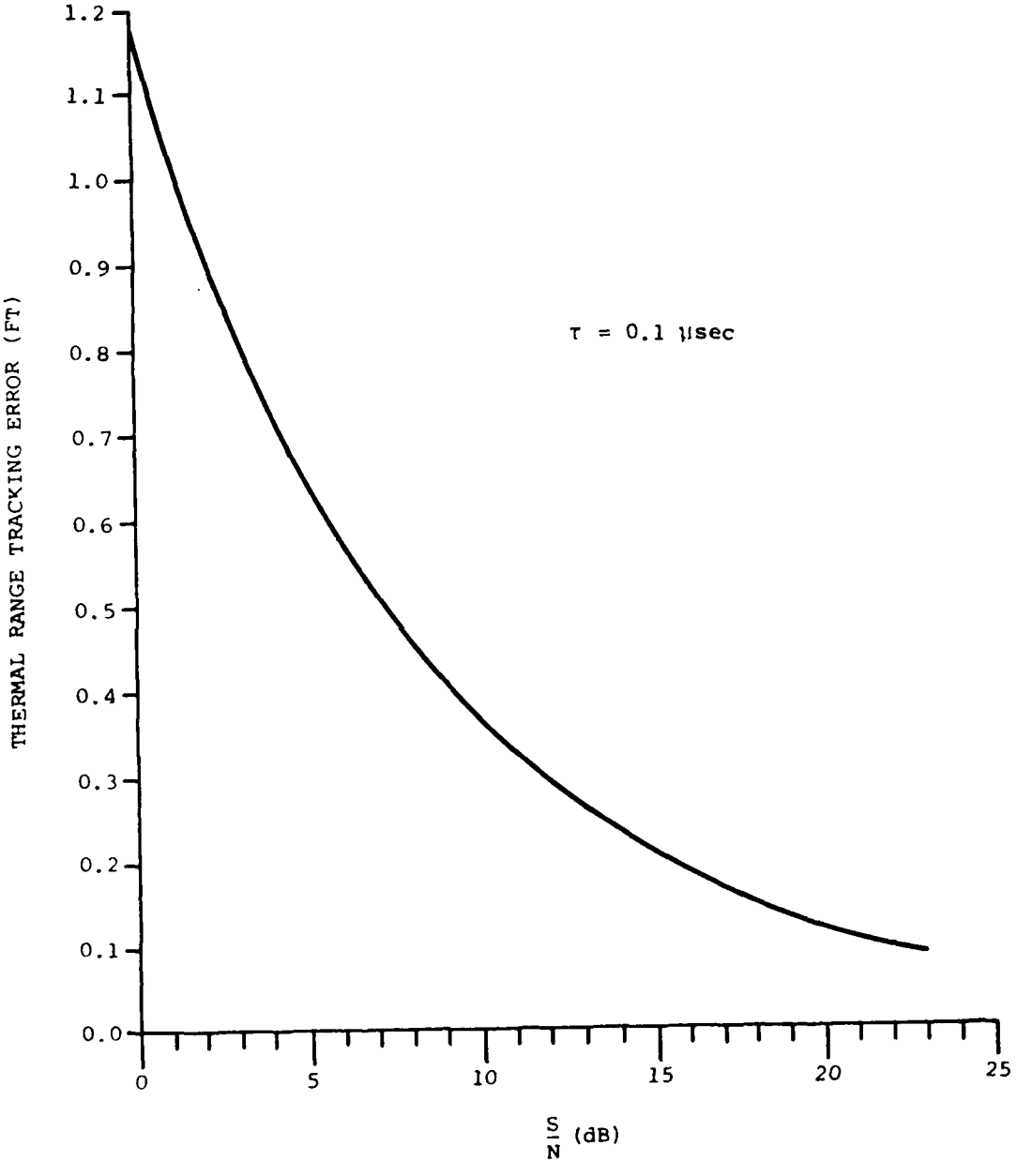

Figure 24. RMS Thermal Range Tracking Error vs S/N
($\tau \approx 0.1$ μsec)

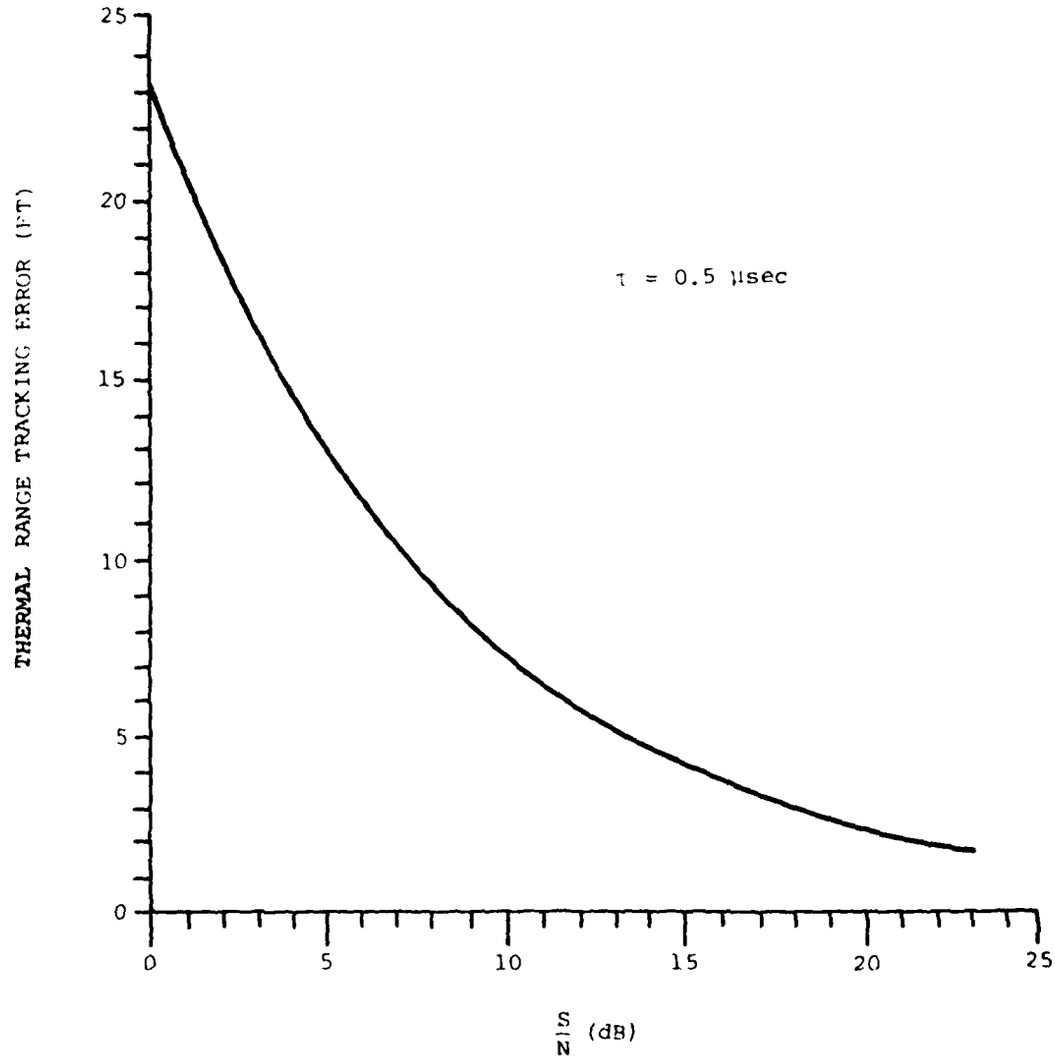

Figure 25. RMS Thermal Range Tracking Error vs S/N
(τ = 0.5 μsec)

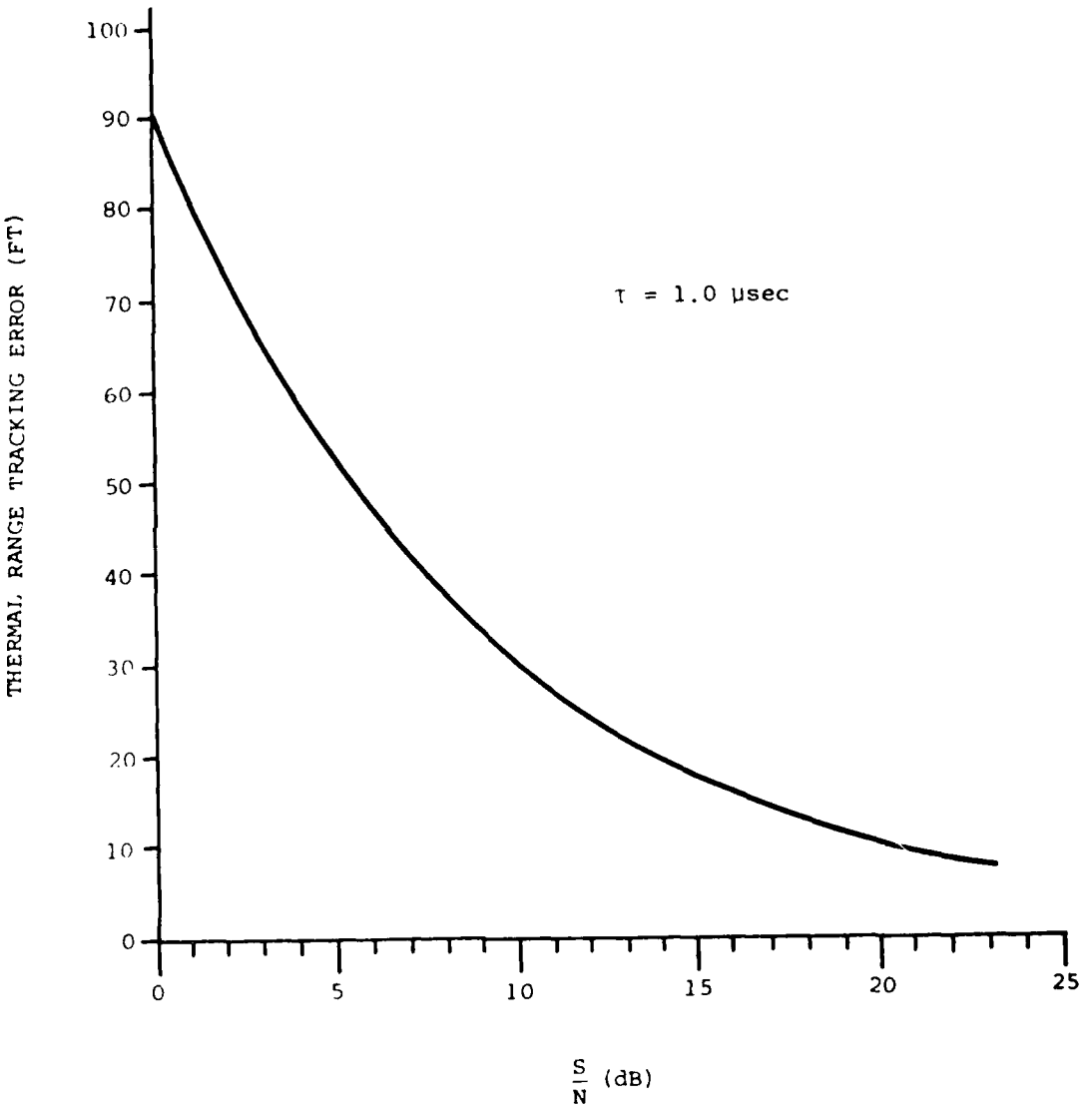

Figure 26. RMS Thermal Range Tracking Error vs S/N
(τ = 1.0 μsec)

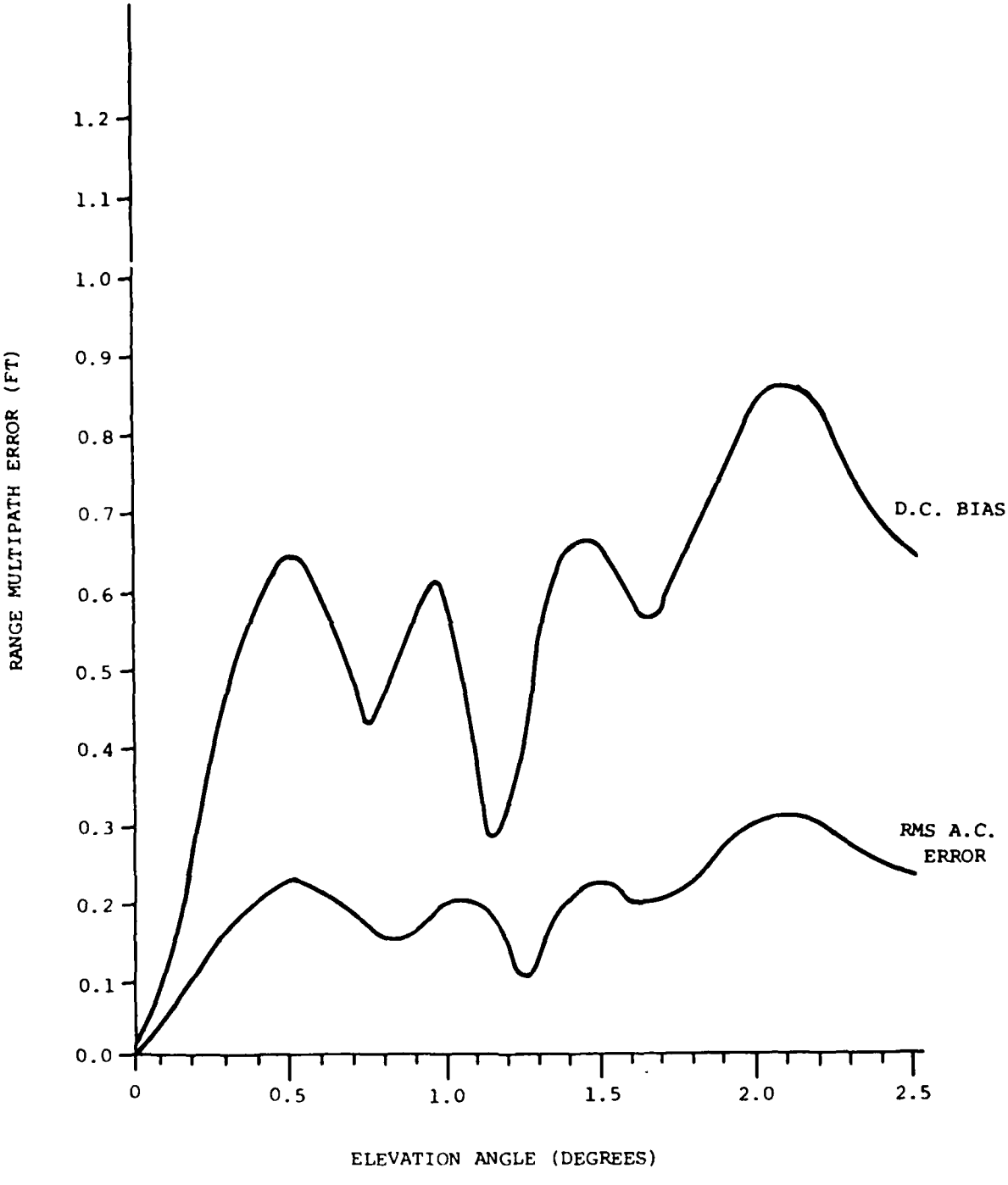

Figure 27. Range Multipath Error vs Target Elevation Angle

Table 4. RMS Range Tracking Error at Low Elevation Angles

	RMS Range Error (ft)	
Pulsewidth (μsec)	Short Range R = 0.5 nmi	Long Range R = 15 nmi
0.1	1.84	8.37
0.5	7.41	11.03
1.0	29.06	30.18

NOTE: Target elevation angle = 0.5°
S/N = 10 dB

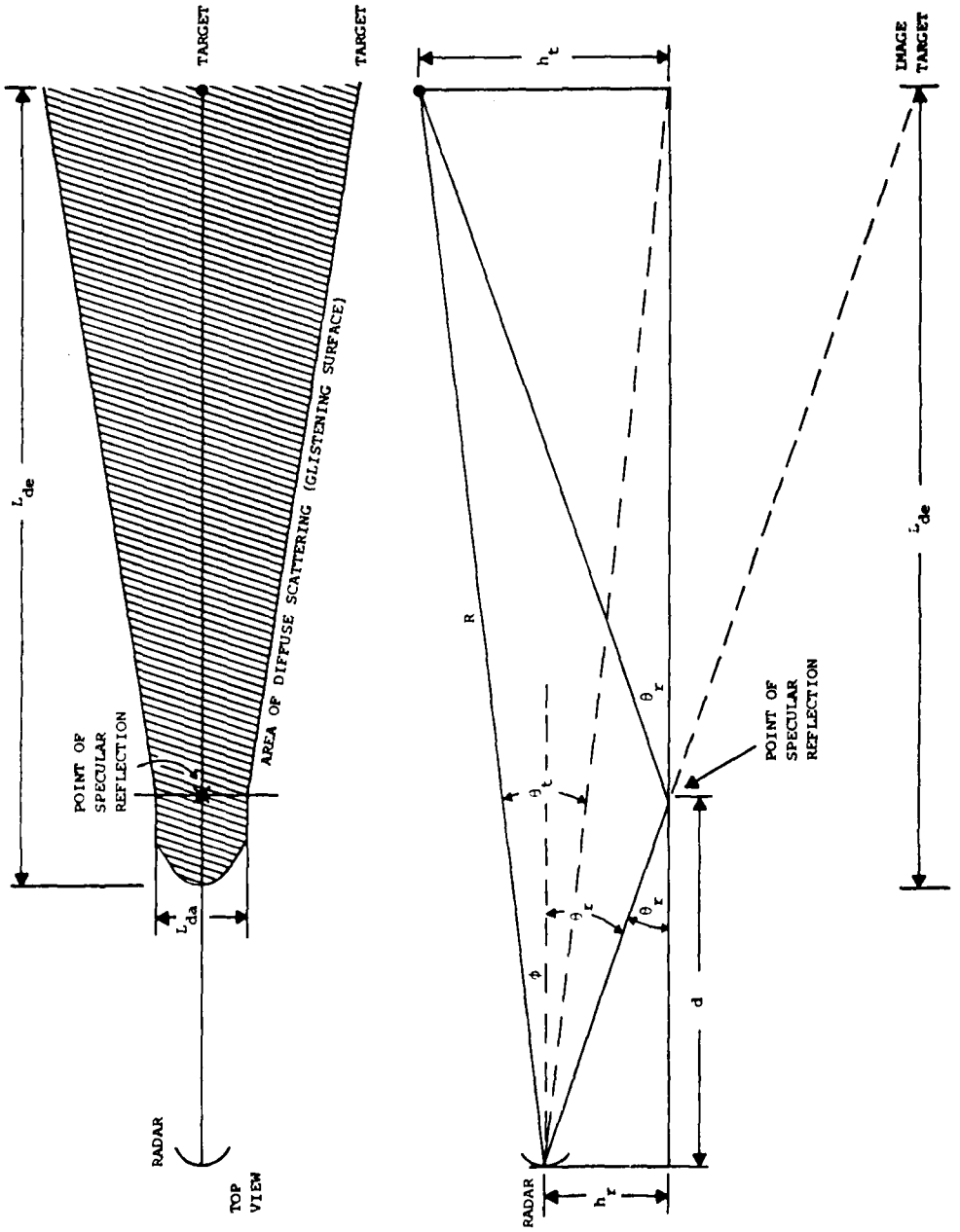

Figure 28. Geometry of Radar and Target Orientation with Multipath Reflections

Table 5. Selected Calculated Parameters for Geometry of Figure 28

R (ft)	θ_t (deg)	d (ft)	θ_r (deg)	ϕ (deg)	θ_{da} (rad)	L_{da} (ft)	θ_{de} (rad)	L_{de} (ft)
1000	5.71	230.8	7.41	4.00	0.030	6.92	0.400	838
2000	2.86	461.5	3.72	2.00	0.015	6.92	0.350	1677
3000	1.91	692.3	2.48	1.34	0.010	6.92	0.330	2516
4000	1.43	923.1	1.86	1.00	0.0075	6.92	0.325	3354
5000	1.15	1153.8	1.48	0.80	0.006	6.92	0.320	4190
6000	0.95	1384.6	1.24	0.67	0.005	6.92	0.317	5030
7000	0.82	1615.4	1.06	0.57	0.0043	6.92	0.314	5870
8000	0.72	1846.2	0.93	0.50	0.0038	6.92	0.313	6708
9000	0.64	2076.9	0.83	0.45	0.0033	6.92	0.311	7540
10000	0.57	2307.7	0.75	0.40	0.003	6.92	0.310	8384
11000	0.52	2538.5	0.68	0.37	0.0027	6.92	0.309	9223
12000	0.48	2769.2	0.62	0.33	0.0025	6.92	0.308	10060
NOTE: h_r = 30 ft, h_t = 100 ft								
1000	4.00	300	5.71	2.29	0.0210	6.30	0.370	790
2000	2.00	600	2.86	1.15	0.0110	6.30	0.335	1580
3000	1.34	900	1.91	0.76	0.0070	6.30	0.323	2370
4000	1.00	1200	1.43	0.57	0.0053	6.30	0.318	3160
5000	0.80	1500	1.15	0.46	0.0042	6.30	0.314	3950
6000	0.67	1800	0.96	0.38	0.0035	6.30	0.312	4740
7000	0.57	2100	0.82	0.33	0.0030	6.30	0.310	5530
8000	0.50	2400	0.72	0.29	0.0026	6.30	0.309	6320
9000	0.45	2700	0.64	0.26	0.0023	6.30	0.308	7100
10000	0.40	3000	0.57	0.23	0.0021	6.30	0.307	7900
11000	0.36	3300	0.52	0.21	0.0019	6.30	0.306	8690
12000	0.33	3600	0.48	0.19	0.0018	6.30	0.306	9480
NOTE: h_r = 30 ft, h_t = 70 ft								
1000	2.86	375	4.57	1.15	0.0150	5.62	0.350	738
2000	1.43	750	2.29	0.57	0.0075	5.62	0.325	1475
3000	0.95	1125	1.53	0.38	0.0050	5.62	0.317	2213
4000	0.72	1500	1.15	0.29	0.0038	5.62	0.313	2950
5000	0.57	1875	0.92	0.23	0.0030	5.62	0.310	3688
6000	0.48	2250	0.76	0.19	0.0025	5.62	0.308	4429
7000	0.41	2625	0.66	0.16	0.0021	5.62	0.307	5163
8000	0.36	3000	0.57	0.14	0.0019	5.62	0.306	5900
9000	0.32	3375	0.51	0.13	0.0017	5.62	0.306	6638
10000	0.29	3750	0.46	0.12	0.0015	5.62	0.305	7375
11000	0.26	4125	0.42	0.11	0.0014	5.62	0.305	8113
12000	0.24	4500	0.38	0.10	0.0013	5.62	0.304	8850
NOTE: h_r = 50 ft, h_t = 50 ft								

Also shown in Figure 28 is a top view of the points of specular reflection and areas of diffuse scattering (glistening surface) that are encountered with low elevation angle tracking. L_{de} is the length of this glistening surface area measured from the projection of the target on the surface. L_{da} is the width of this area at the point where specular reflection would take place if the surface were smooth. L_{da} increases directly with distance from the radar, because it is generally represented by an angular spread with respect to the radar. The more conventional method of illustration using angular spread is shown in Figure 29 along with the specular reflection case of Figure 30. The glistening surface amplitude is approximately -4 dB at the edges with respect to the center point of specular reflection. Figure 30 shows the discrete point in angular coordinates of the multipath reflection with respect to the radar for the smooth surface case. Figure 29 shows the angular spread of multipath reflections and diffuse scattering for the same geometry of Figure 28, but the surface is rough instead of smooth. An ellipse shaped angular area of diffuse scattering results with major and minor angular axes θ_{de} and θ_{da} respectively. The ellipse of Figure 29 would not intersect the horizon if the reflecting surface (sea) was much smoother, or the elevation angle to the target was larger. The low elevation angle used in the calculations is much less than the average surface roughness which is characterized by the RMS surface slope σ_α. This is the condition that causes this ellipse to intersect the horizon even for a very calm sea (almost smooth surface). The RMS surface slope is a function of wind velocity and is typically 0.05-0.25 radians (see reference 3). The 0.05 RMS surface slope is a very calm sea or almost smooth condition. This RMS surface slope increases very quickly to 0.15 radians which corresponds to a wind velocity of 10 knots, and then levels off with a more gradual increase to 0.25 radians which corresponds to a wind velocity of 30 knots. Figure 29 is a good representation of the conditions under which the millimeter wave radar was tested. Table 5 represents the different target locations in range and how all of the other defined parameters would change for a target moving out in range and changing its elevation angle.

The glistening surface encountered for a moderately rough surface is characterized by random scattering. This scattering combined with the random occurring specular components from the irregular surfaces creates the multipath conditions that affect radar tracking performance. At very low elevation angles the intense scatters at the horizon tend to be specular in nature. Even this specular nature tends to be random in time due to the randomness of the irregular surface with time. The radar sees both the image and the target. The randomness of the appearance of the image due to reflection and scattering confuses the radar and causes it to lose track.

If ρ_0 is the reflection coefficient for a smooth surface, the coefficient of specular reflection for an irregular surface is given by $\rho = \rho_s \rho_0$, where ρ_s is the specular scattering factor and represents the RMS value of the field which is reflected without being perturbed by the surface irregularities. The expression taken from reference 2 for this scattering factor is:

$$\bar{\rho}^2_s = \exp\left[-\left(\frac{4\pi\sigma_h \sin\gamma}{\lambda}\right)^2\right]$$

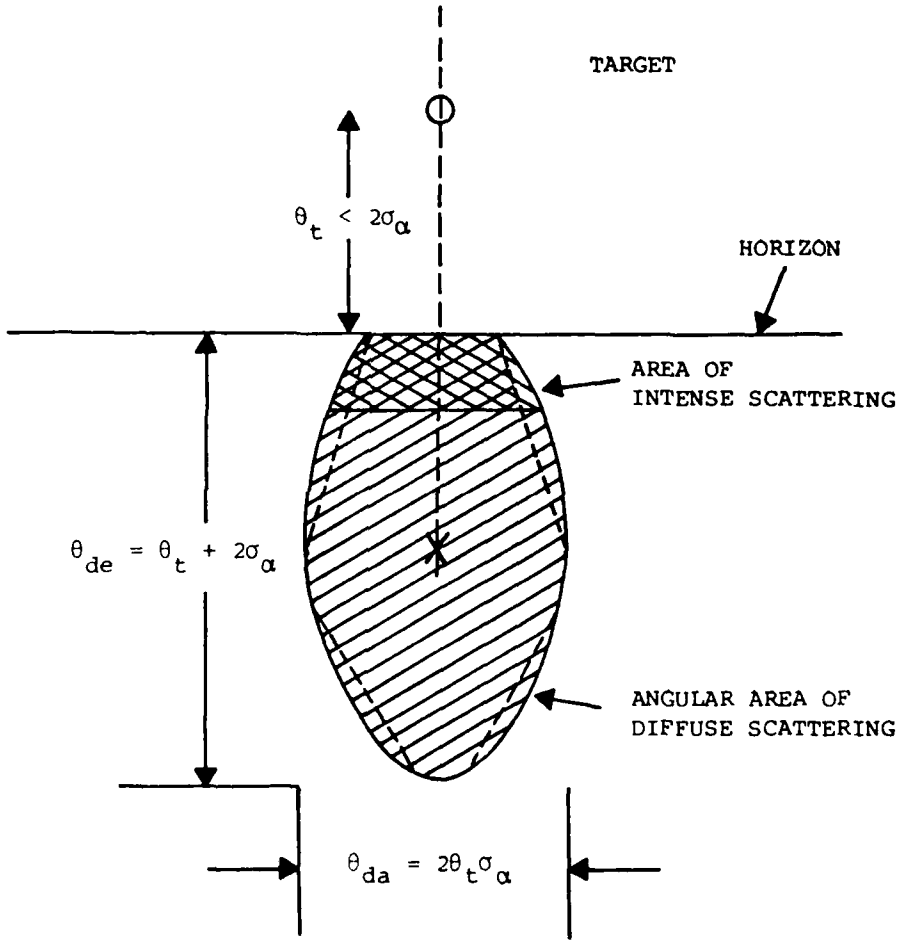

Figure 29. Angular Spread of Multipath Reflections for a Long Range Target and Low-Sited Radar with a Rough Reflecting Surface (Diffuse Scattering)

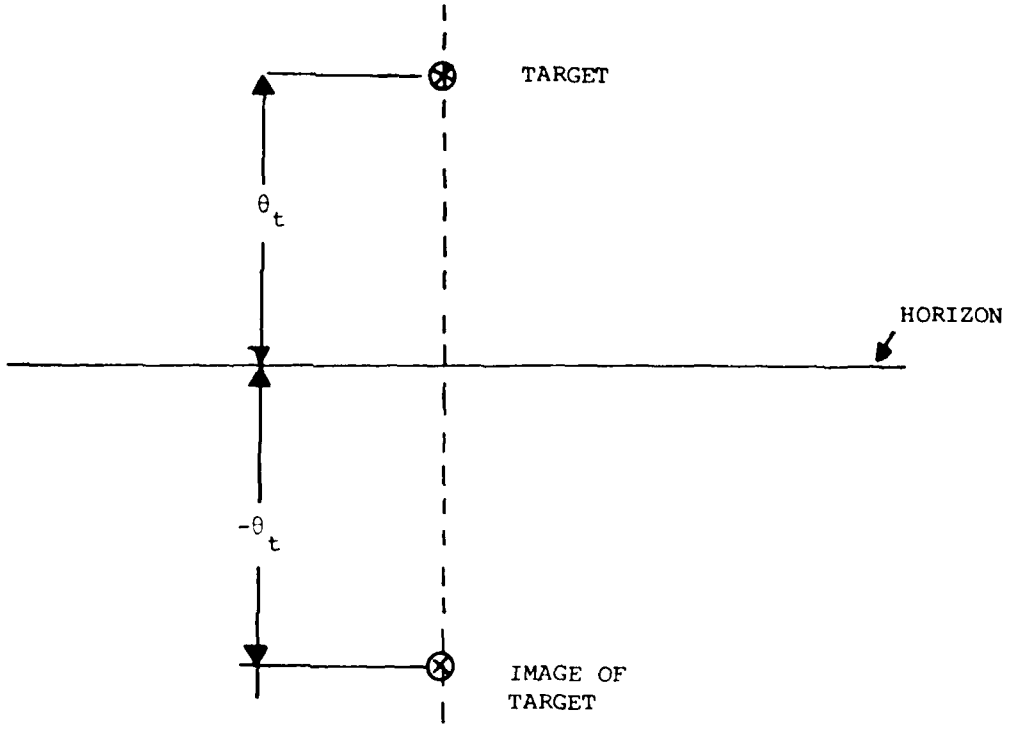

Figure 30. Angular Spread of Multipath Reflections for a Long Range Target and Low-Sited Radar with a Smooth Reflecting Surface (Specular Reflection)

where

$\bar{\rho}^2_s$ = mean square value of ρ_s

σ_h = RMS deviation in surface height

γ = grazing angle

λ = wave length

The grazing angle is equal to the target elevation angle when the flat-earth approximation is valid. A surface is considered rough when $\bar{\rho}^2_s \leq 0.5$ which by the above expression for ρ_s is equivalent to:

$$\frac{\sigma h}{\lambda} \sin\gamma \geq 0.065$$

This expression is equivalent to the Rayleigh criterion for surface roughness. The grazing angle above which a surface appears rough can be calculated with this expression.

Table 6 contains the results of these calculations for three frequencies and a variety of sea states. When the grazing angle exceeds twice the angle calculated using the above expression, the specular component becomes very small, and the reflection coefficient depends on the diffuse scattering factor ρ_d, such that $\rho = \rho_0 \rho_d$. Figure 31 from reference 2 shows the variation of the scattering factors as a function of RMS surface roughness. It can be seen from Table 6 and Figure 31 that if either the surface becomes rougher or the elevation angle to the target is increased, the scattered energy back into the receiver becomes more diffuse and the radar will be able to track the target.

Table 6. Maximum Angles for Specular Reflection at Different Radar Frequencies and Sea States

Sea State Number	Wave Height (meters)	RMS Height σ_h (meters)	Critical Angle, γ_{max} (deg)		
			λ = 0.1 m f = 3 GHz	λ = 0.03 m f = 10 GHz	λ = 0.0086 m f = 35 GHz
1	0-0.3	0.065	> 5.7	> 1.72	> 0.49
2	0.3-1.0	0.065-0.21	1.77-5.7	0.53-1.72	0.15-0.49
3	1.0-1.5	0.21-0.32	1.16-1.77	0.35-0.53	0.10-0.15
4	1.5-2.5	0.32-0.54	0.69-1.16	0.21-0.35	0.06-0.10
5	2.5-4.0	0.54-0.86	0.43-0.69	0.13-0.21	0.04-0.06
6	4.0-6.0	0.86-1.30	0.29-0.43	0.086-0.13	0.025-0.04

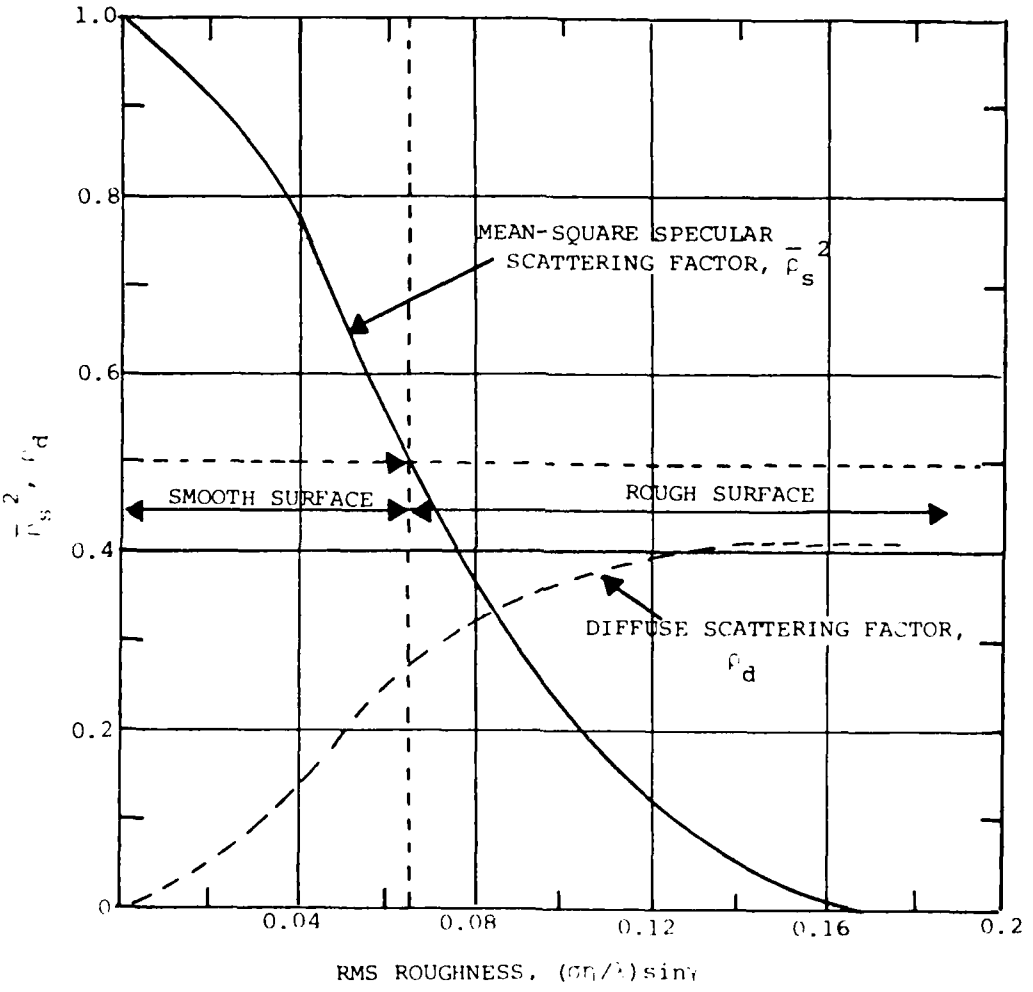

SCATTERING FACTORS VS ROUGHNESS (AFTER BECKMANN AND SPAZZICHINO). (REFERENCE 2)

Figure 31. Scattering Factors vs Surface Roughness (see reference 2)

Since the objective is to detect and track targets at low elevation angles, it is desirable to have a rough surface for as small an angle as possible. The expression for surface roughness indicates that a shorter wavelength would increase the effective surface roughness. This is one of the advantages of using millimeter wavelengths for low angle detection and tracking. The millimeter wavelengths also allow narrower beamwidths for a given aperture size than lower frequencies in addition to narrower monopulse difference patterns for better angle tracking.

PERFORMANCE IN AN ECM ENVIRONMENT

When operating in an ECM environment, the increased immunity to jamming of millimeter wave radar is due to the narrow antenna beamwidth possible with physically small apertures. Another benefit stems from the present state-of-the-art in millimeter wave generation and amplification. Very high-power transmitters and amplifiers are not readily available and due to the state-of-the-art at millimeter wave frequencies, expendable jammers are not yet a reality at 35 GHz. Using postulated jammer characteristics whose numerical values are based on current state-of-the-art hardware, an analysis was performed to determine the effective detection performance in the presence of a stand-off jammer (SOJ) and a self-screening jammer (SSJ). The SOJ will not be a problem, because the jammer would be well beyond the millimeter wave radar maximum detection range in a tactical situation with conventional SOJ procedures. The SSJ case, however, is a problem because the self-screening range is much less than a mile for worst case. The radar must therefore depend on its narrow antenna beamwidth and low side lobes, or resort to a more sophisticated technique of frequency agility to counter the SSJ. The addition of frequency agility to the system will increase its immunity to jamming in an ECM environment. Using the appropriate parameters of the 35-GHz monopulse radar, a minimum frequency agile bandwidth was calculated based on references 4 through 8. This bandwidth will be necessary to produce the requisite performance and to achieve a 6-8 dB increase in S/N. A minimum bandwidth of 200 MHz appears adequate. An additional advantage of increased clutter rejection is also obtained with frequency agility.

PROBLEMS ENCOUNTERED IN DEVELOPMENT AND TESTING OF THE MILLIMETER WAVE RADAR

TRANSMITTER

The high voltage section in the modulator is enclosed in a sealed oil reservoir. This oil reservoir in the millimeter wave radar was constantly plagued with oil leaks. The oil leaks originate from the problem of fabricating a metal solder sealed container that can hold an essentially incompressible fluid under a wide temperature range. Specially designed bellows are used for pressure compensation due to thermal expansion, but if these are not adjusted correctly, the expansion of fluid with temperature can cause leaks in the sealed container. In addition to the outside environment, the high voltage section also generates its own heat.

The oil is also used as a coolant in addition to being a high dielectric fluid. The oil leak aggravates an already critical problem of high voltage regulation in the modulator, that depends on the thermal and dielectric properties of this oil. The small variation in the high voltage section produces significant variations in the millimeter wave output frequency beyond the capability of the AFC circuit to maintain the proper IF. Even after thermal stabilization is achieved there are still significant changes in the millimeter wave output frequency due to high voltage pulse height stability.

The inverted coaxial magnetron design with its much larger cathode assembly has a long warm-up time (as long as 30 min), before dimensional stability is obtained in the cavity for sufficient frequency stability. This warm-up time requires that the high voltage pulse be applied in addition to the filaments because application of the high voltage pulse to the tube causes significant additional heating of the tube. The RF output frequency of the tube was also different for different PRFs and pulsewidth, because of the oil leak compounding the high voltage regulation problem. After repairing the high voltage section of the modulator and sealing the container, the frequency stability improved significantly. The millimeter wave frequency output is now stabilized after 30 min of warm-up with the high voltage on.

A later failure in the filament circuitry of the modulator caused poisoning of the cathode in the magnetron. This occurs when the high voltage is applied to the magnetron tube before the cathode has sufficient time to warm up. The high field strengths in a tube with a cold cathode causes ion bombardment of the cathode. The cathode is then poisoned and additional ions are present in the tube vacuum. The magnetron was no longer operative and had to be replaced. The new magnetron required at least 50 hours of burn-in time before it could deliver RF power at full PRF output. After burn-in of the new magnetron, the transmitter worked with stable RF and power output.

DUPLEXER

The operation of the duplexer was covered previously in the discussion section. The basic problem in the operation of this type duplexer originates from the fact that the synchronizer that controls the switching of the latching ferrites from low to high and back to low attenuation states during radar operation, also predicts when the receiver needs to be protected. The synchronizer bases this need on a trigger pulse that occurs exactly at the same time as the transmitter tube RF output pulse (main bang). The latching ferrite device operation does not sense RF power to initiate receiver protection as would a receiver protected by a transmit-receive (TR) tube or limiter. The receiver with latching ferrite protection is not protected against occurrence of an extra pulse within the normal pulse repetition interval (PRI).

The amount of delay that occurs in the modulator between the transmitter modulator initiation pulse and the actual RF output pulse prohibits the instantaneous switching of the latching ferrites with this transmitter modulator initiation pulse. This delay is approximately 8, 12, and 16 μsec for the 0.1, 0.5, and 1.0 μsec

pulsewidths respectively. This delay represents the charging time for the pulse forming network in the modulator.

The synchronizer is therefore a timer that starts counting when the transmitter initiation pulse is input to the modulator, and after a fixed delay, depending on pulsewidth, the synchronizer switches the ferrites to the high attenuation state for the time interval when the main bang is supposed to occur. There is a sufficient margin on either side of this time interval to assure receiver protection if the transmitter fires regularly with a constant PRI, but not if the magnetron adds a pulse between normally occurring pulses. The occurrence of an extra pulse could easily destroy the mixer diodes at full power output. The testing was performed using a 40-dB reduction in transmitter power output. If the receiver was not protected for a limited number of pulses, the mixers could handle the power levels for a certain period of radar operating time. One pulse at full power without receiver protection would have destroyed the mixer diodes instantly.

Prior to the beginning of the test program a large number of mixer failures occurred even at low power during calibration runs. It was discovered that the latching ferrite trigger pulse amplifier was not delivering a sufficient pulse to switch the ferrite cores. Further investigation located a mechanically fractured resistor (not electrically burned) in the pulse amplifier. This was replaced and normal operation was restored with the ferrites switching as required. A later latching ferrite trigger amplifier failure occurred that was caused by a screw in the latching ferrite trigger amplifier box that shorted the output circuit. This failure burned out the output stage and required replacement of several electronic components.

A severe electromagnetic interference (EMI) problem exists due to the high voltage and current levels switched in the modulator. This is also a mechanism for false triggering of the synchronizer despite heavy EMI filtering in the modulator and synchronizer.

The duplexer worked well throughout the test program, but still has the drawback that it cannot protect the receiver from extra pulses that do not occur at the correct PRI. A TR-limiter type device is strongly recommended for replacing the latching ferrites in the duplexer. They are presently available at 35 GHz and capable of handling power levels as high as 130 kW peak and 52 W average.

Using a circulator in the standard radar duplexer configuration in the block diagram of Figure 1 to direct power from the transmitter to the antenna, the TR-limiter is not required to withstand the full transmitter output power. Only 11 percent of the peak and average transmitter power will be reflected back into the TR-limiter, assuming an antenna voltage standing-wave ratio equal to 2:1.

MIXERS

The Schottky Barrier diode mixers in the receiver had a very high failure rate because of both mechanical and electrical problems. A 5-Vdc level across the diode terminals will destroy the diode. All waveguide and coax connections to the mixer must be at the same potential before bringing them in contact with the

mixer. Static electricity will also damage diodes if the Sharpless wafers are removed from the mixer housings. Inside the mixer housings these wafers are protected from static discharge. Excess RF power will also damage the diodes. The damage levels are +20 dBm continuous wave and +28 dBm peak (0.001 duty factor). These are the manufacturer's absolute maximum ratings. The mixers will take short bursts of RF energy above these maximum levels for a limited number of times (pulsed case) or a very short time interval (continuous wave case).

The mechanical failures of the diode mixers can be attributed to the non-hermetic seal of the mixer package and the construction of the Sharpless wafer shown in Figures 32 and 33. The Sharpless wafer is essentially a diode mounted in a reduced height waveguide section with connections to couple the output to the IF connector and the other wafer in the mixer that forms the balanced pair. The whisker wire from one pin of the wafer is 0.001 in. in diameter and is sharpened like a pencil on one end. This end is pressed into a single diode on the semiconductor chip which contains approximately 1000 diodes in a matrix array that are 5 microns in diameter and located on 10 micron centers. The wire contacts only one diode in a point contact diode type of configuration. The wire is under a slight tension supplied by the double bend shown in Figures 32 and 33. This assembly is subject to failure in moderate mechanical vibration and shock environments. It was the first method of producing very low noise diode mixers at millimeter wave frequencies. This technique can be tracked back about 20 years. Recently, an improved technique was developed for mixers. It involves using the beam lead diode configuration in a specially designed package. Reliable low noise beam lead diodes at millimeter wave frequencies are presently available for mixers.

The mixer problems related to the lack of environment protection was also discovered during the testing of the radar. Deposits from the salt air environment, smoke stack sediment from a power station near the test site, and assorted foreign matter were found in the Sharpless wafers and mixer housings. These materials were discovered on the surface of the semiconductor chip and the microstrip transmission line inside the mixer by personnel in the U14 Microelectronics Facility at NSWC. The mixers that had severe amounts of these constituents had been removed from the radar, because they exhibited poor noise figures.

Personnel from the U14 Microelectronics Facility and the Radar Engineering Branch, developed techniques that could repair mixers damaged by foreign deposits, mechanical environment, or excess electrical power (static or RF). Hermetically sealing the mixer housings can solve this problem.

The techniques developed saved both time and money over the alternative of returning the mixers to the manufacturer for repair. The most significant saving was in time, because of the high rate of failure of the mixers. The in-house developed techniques required less than 4 hours to repair and test a set of mixers. Returning the mixers to the manufacturer for repair would require a minimum of 2 weeks.

It is recommended that the mixers be replaced with the new beam lead diode types that are more rugged mechanically and are hermetically sealed. The static and RF power limitations are still present with this configuration.

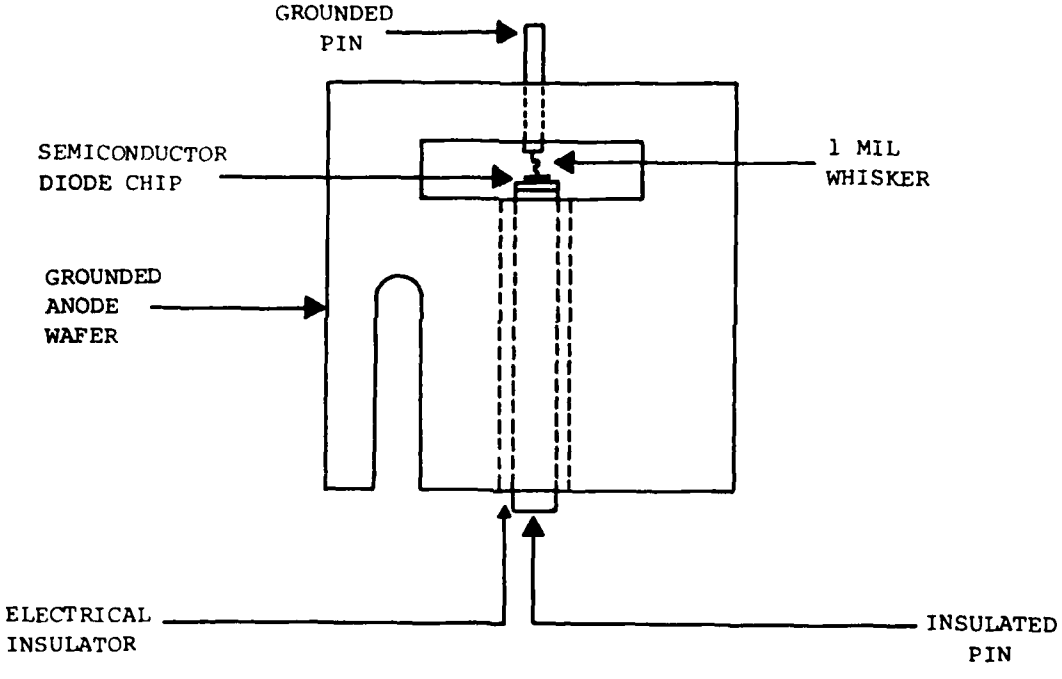

Figure 32. Drawing of a Modified Sharpless Grounded Anode Wafer

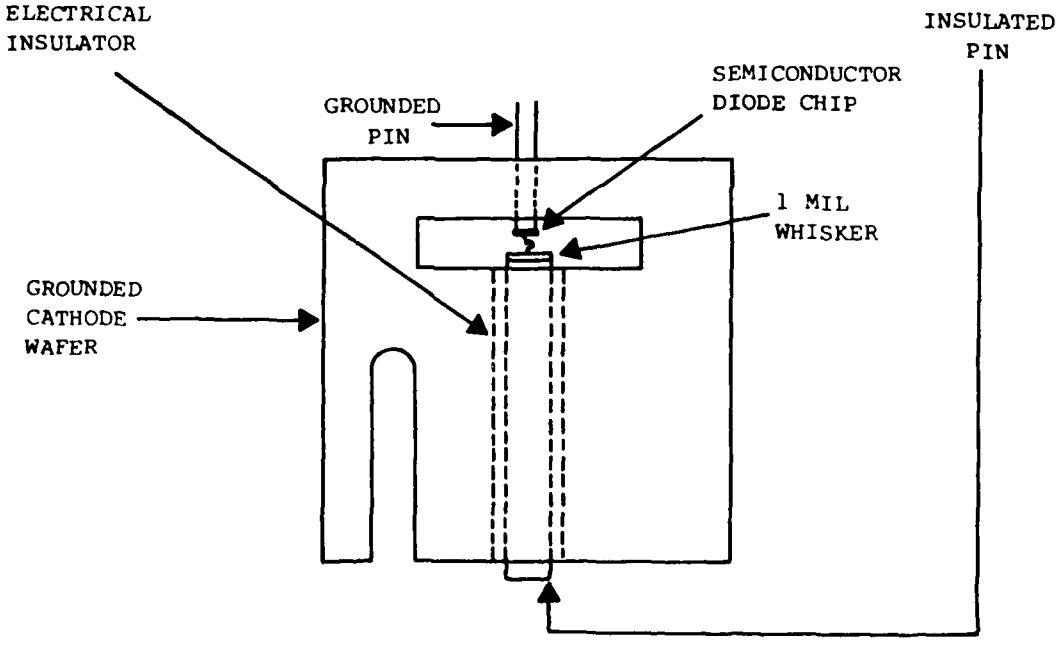

Figure 33. Drawing of a Modified Sharpless Grounded Cathode Wafer

CONNECTION PROBLEMS IN THE RADAR ELECTRONICS

The cabling and interconnections in the radar electronics mounted on the pedestal carry power supply voltages and returns, logic control signals, analog signals, and RF signals. The motion of the pedestal in the elevation plane during tracking can create a severe mechanical shock environment for the cable connections causing failures. The moist air environment also caused problems with the cable connections and card edge connectors. A large number of radar failures could be traced to connector and cable failures, particularly in the video processor.

It is recommended that the radar electronics be enclosed in a weather tight housing. In addition, it is also recommended that the video processor card cage be scrapped and a new assembly built with a weather and RF tight configuration similar to that used for the MIF. This construction is typical of that used at RF with subminiature threaded RF connectors for signal cables and feed through terminals for power supply connectors. Each of the video processor circuit boards would be self-contained in its own housing. This would minimize environment problems, eliminate card edge connector problems and reduce EMI. The EMI environment is very severe with the high voltage pulse levels of the transmitter and the ultra-fast pulse circuits of the video processor. Noise levels and sensitivity in the video processor would also improve. It was discovered during the testing that the logarithmic amplifier could not be used over the full extent of its dynamic range, because of the high noise level in the video processor. Subminiature threaded RF connectors for signal carrying cables between circuit board modules would be far superior to the unshielded card rack interconnections now used.

GUNN DIODE DRIFT PROBLEMS

Gunn diode oscillators are stable sources of continuous wave millimeter wave frequencies in a fixed temperature environment, but they are characterized by a large drift in output frequency versus temperature. It is therefore necessary to use a temperature stabilizing device with the Gunn diode oscillator to stabilize frequency. The magnitude of the change is -1 MHz/°F for a Gunn diode oscillator at 35 GHz. The temperature stabilizing device attached to the oscillator on the millimeter wave radar failed during testing, and the oscillator moved to a frequency of operation where it could not be controlled by the AFC circuitry. The Gunn oscillator in the radar is varactor tuned and its frequency is controlled by a dc voltage determined by the radar AFC circuit. The Gunn diode has a limited tuning range over the voltage range allowed by the varactor. A 20-MHz change corresponds to a 2-V tuning excursion on the control voltage. The voltage range allowed by the varactor is +0.6 to -10 V.

As the Gunn diode got colder the frequency would go up and the AFC would compensate for this by reducing the negative voltage towards zero to a positive voltage. This voltage could not go past +0.6 V. Even at this voltage the frequency was too high to maintain the 60-MHz IF offset from the transmitter frequency.

The heater was repaired and normal operation was restored for moderate changes in environmental temperatures.

A further improvement in performance was obtained by enclosing the Gunn diode oscillator and heating element in a thermal container, so that the Gunn could be kept sufficiently warm even in very cold weather (below +20°F) and high winds. The tuning curve would then stay in the appropriate voltage and RF range.

TEST PROGRAM

EXTENT OF TESTING

The initial test program for the millimeter wave radar was successfully completed in December 1979 at Station 9, Dahlgren. The test plan for this program is contained in Appendix A. Very low elevation angle tracking data of surface and air targets was collected using the millimeter wave radar. The radar was operational and ready for testing on 7 November 1979, and the first successful tracking test was performed on 8 November 1979 using a range boat as a target. Approximately 2 hours of tracking data were recorded. Range boat maneuvers included: crossing, receding, approaching and zig-zag courses with and without corner reflector augmentation. The elevation angles used during the test were 0 to -1° which will produce maximum multipath conditions for the radar and target geometries of the test site.

An additional 2 hours of range boat tracking data was obtained on 11, 12, and 14 December 1979. Tracking data of both low and high angle air targets (helicopter) were also obtained on 12 and 14 December 1979. The elevation angles used for the air targets were +8° to approximately +0.2° with the majority of data in the low angle tracking category of +2 to 0.2° region. The helicopter maneuvers included: approaching, receding, crossing, turning, and zig-zag target courses both with and without corner reflector augmentation. The target course geometries with the helicopter were picked for producing maximum multipath conditions. A limited amount of test data was reduced and is presented here with test results and conclusions.

RESULTS AND CONCLUSIONS

A large volume of data was collected with the millimeter wave radar. Many duplicate runs were made to verify the behavior of the radar. All data followed the basic trends described below. The best runs were reduced to obtain the graphs shown in this section. Two types of weather conditions were present during the tests which differed basically in sea state. One set of data was taken for calm conditions and the other approximated sea state two. During the test program the

angle tracking errors from the radar were measured and recorded as a function of target evaluation angle. The target aircraft started initially at a short range and proceeded out across the river, directly away from the radar at a fixed altitude and constant speed. As the range increased the angle decreased. Figure 34 is a plot of the raw data sampled every 0.1 sec. This data was obtained by recording the position of the track symbol with respect to the target location on the video monitor. The error is cyclic and grows to a large value before the radar loses track. This loss of track occurs because the large peak excursions force the antenna position such that the target location is outside of the antenna difference pattern main null. The steering command derived by the radar reverses sign outside of this region, driving the antenna off of the target. Figure 22 from the analysis section is a plot of RMS multipath angle tracking error versus elevation angle and was plotted from points that were calculated using radar antenna patterns and other radar parameters. The data from Figure 34 can be made to correspond to Figure 22 by taking the RMS value of the cyclic variation from Figure 34 and plotting it versus the elevation angle (see Figure 35). The angular range of data from Figure 34 is much smaller than that from Figure 22. By comparing the absolute magnitude of this measured data tracking run and others with the theoretically calculated curve, the magnitude of the reflection coefficient can be determined.

Some radar cross-section data can also be obtained, because the receiver and logarithmic amplifier channel were calibrated. The target size of the corner reflector was also known. The radar corss-section of the CH46 helicopter was measured. Its cross-section of a beam aspect was found to have a mean value of 20 square meters and the nose aspect of a mean value of 4 square meters.

The most significant data collected during the tracking runs was the lowest elevation angle at which the radar could still maintain a good track. The lowest angles at which tracking could still be maintained varied between 0.23-0.37°. Some of these angles are less than the angle of 0.33° predicted by theory. This result is probably a result of the diffuse scattering characteristics of the radar energy from the surface of the water. The 0.33° is based on what elevation angle causes the lower peak of the elevation plane difference pattern to enter the water. This is also a function of radar and target geometry. The quality of the helicopter tracking improved for sea state two as compared to the calm sea condition.

The boat tracking runs showed extremely low angle tracking of the corner reflector, but were not as informative as the helicopter runs. The helicopter runs better simulated the threat of low angle flyers.

The corner reflector mounted on the boat has an image that is displaced under the surface of the water exactly the same distance that the reflector is elevated off the water. In addition, the boat hull has a significant radar cross-section. When all of these targets are superimposed, there is a tendency for the radar to track the boat hull for smooth sea states, because the superposition of all three has a higher value at the center of the angle formed with respect to the radar by the corner reflector and the corner reflector image. The center of this angle corresponds to the hull (see Figure 36). The center of gravity or strongest center

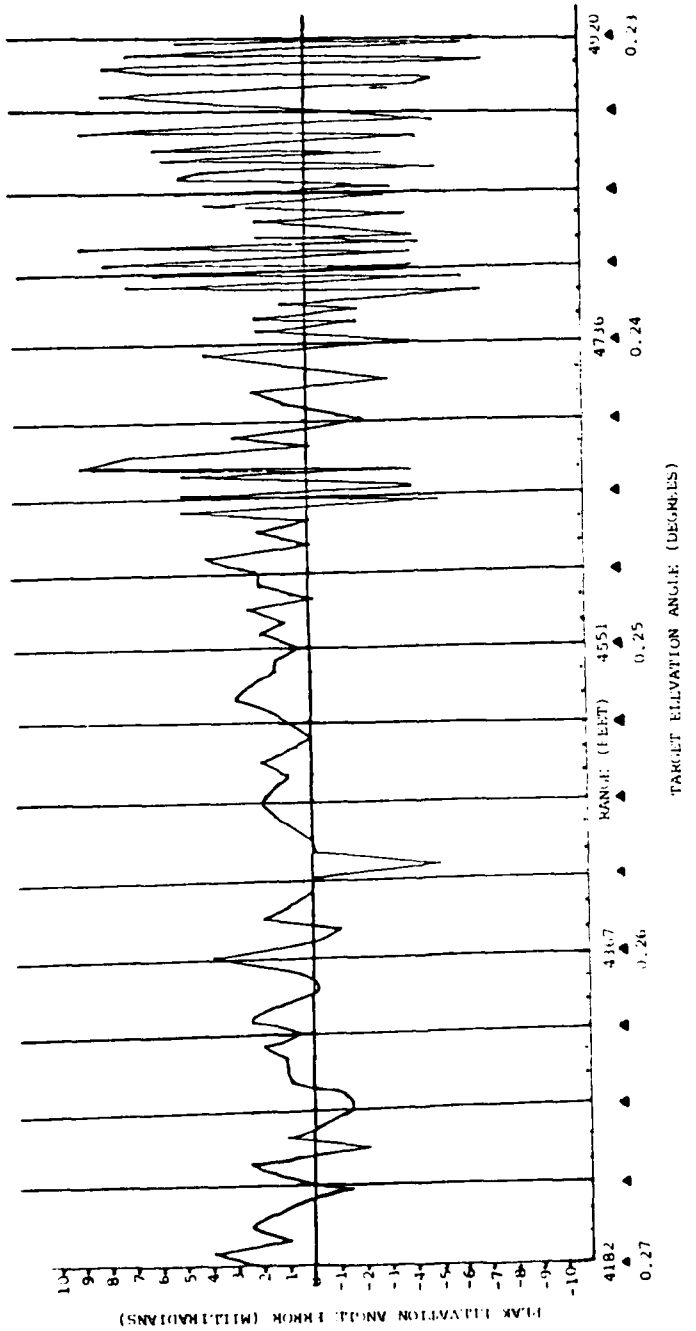

Figure 34. Total Measured Elevation Angle Error vs Range as Target (CH46 Helicopter) Moves Away from Radar

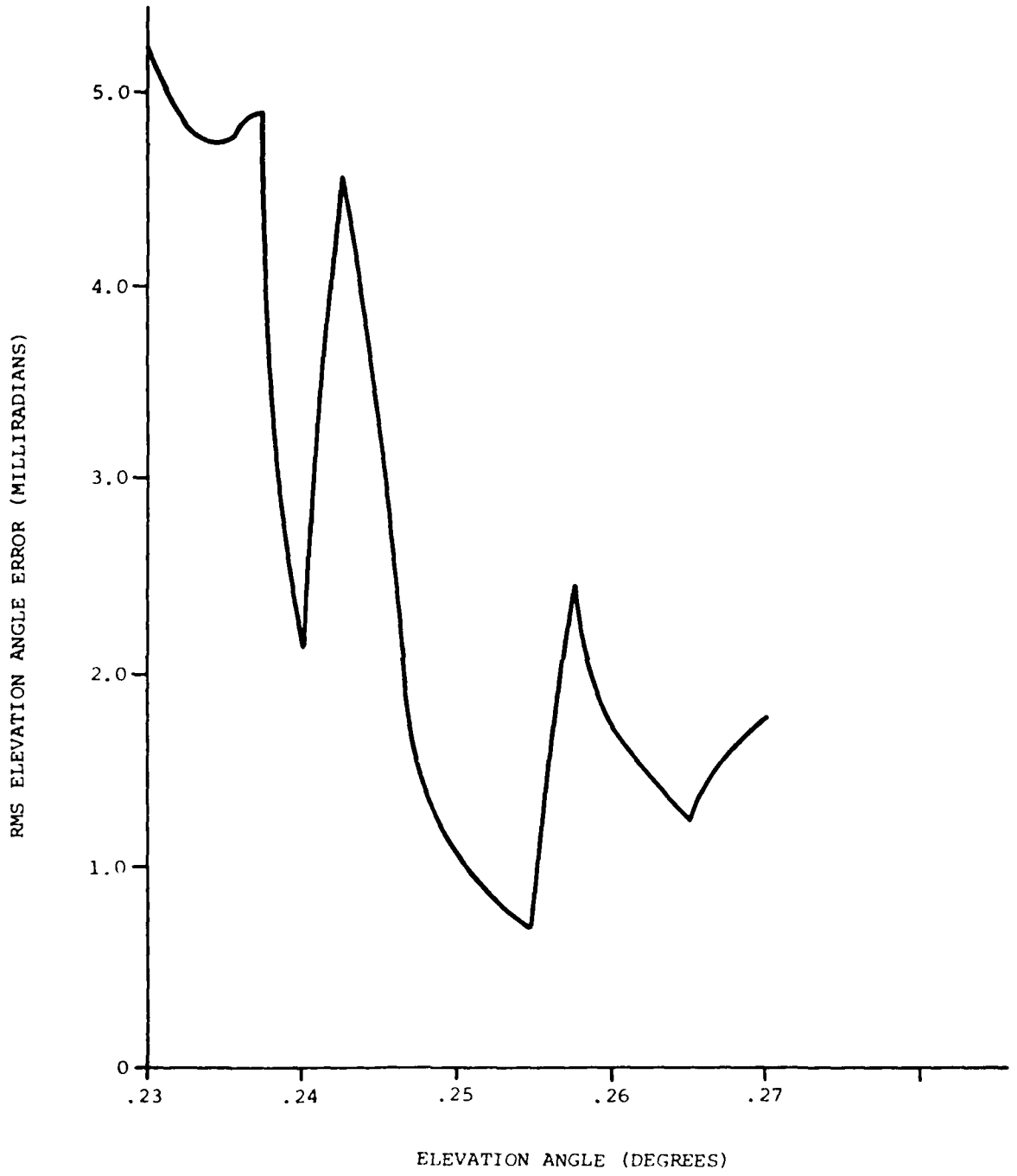

Figure 35. RMS Elevation Multipath Angle Error vs Target Elevation Angle

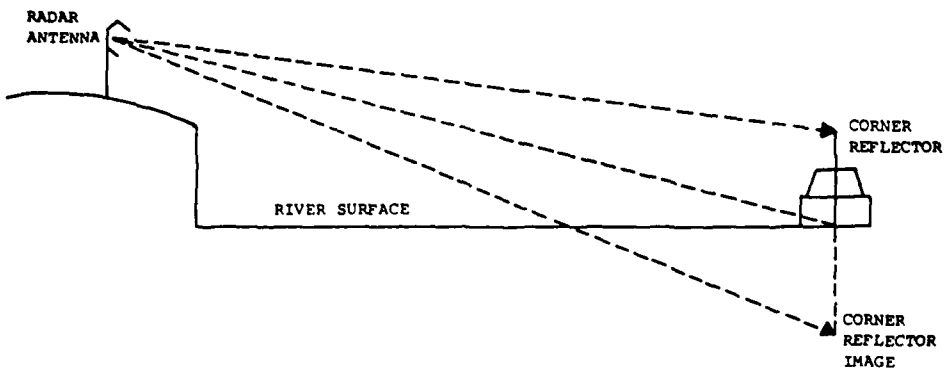

Figure 36. Radar and Boat Target Geometry

of track is on the hull. For a moderately rough sea the surface scattering is more diffuse so the image of the corner reflector has less strength and the center of track shifts to between the hull and corner reflector target. For target tracking runs without the corner reflector augmentation, the radar tracked the hull but had a large glint term in azimuth when viewing a beam aspect. The elevation term was small, because the geometric extent of the target was small in that coordinate and the image of the target was very close to the target in angle.

The tracking test results of the millimeter wave radar are promising. A higher millimeter wave frequency than 35 GHz would probably show better tracking results due to the Rayleigh roughness criterion and the theoretical diffuse scattering predictions. A definite improvement at 35 GHz could be obtained by increasing the antenna aperture linear dimensions by only a factor of 2. This would halve the beamwidth.

In conclusion, the millimeter wave radar system tests indicate this type of radar can fulfill the low angle tracking requirements of the surface Navy.

REFERENCES

1. G. E. Layman, N. DeMinco, and J. H. Brundage, *An Analysis of the Gain and Phase Imbalances for the Millimeter Wave Monopulse Radar Receiver*, NSWC/WOL internal report.

2. P. Beckmann and A. Spizzichino, *The Scattering of Electromagnetic Waves from Rough Surfaces*, Macmillan Co., New York, 1963, Section 5.4.

3. D. K. Barton and H. R. Ward, *Handbook of Radar Measurement*, Prentice Hall, 1969.

4. E. W. Beasley and H. R. Ward, *A Quantitative Analysis of Sea Clutter Decorrelation with Frequency Agility*, IEEE Trans. on AES, May 1968.

5. J. J. Croney, "Improved Radar Visibility of Small Targets in Sea Clutter," *Radio and Electronic Engineer*, September 1968.

6. Goran Lind, *Reduction of Tracking Errors with Frequency Agility*, IEEE Trans. on AES, May 1968.

7. *On the Improvement of Detection Range Using Frequency Agile Techniques*, Boeing Report D6-6835, 1964.

8. H. K. Ray, "Improving Radar Range and Angle Detection with Frequency Agility," *Microwave Journal*, May 1966.

9. L. M. Black, G. E. Layman, J. W. McCorkle, and N. Deminco, *SEATRACKS: A 35-GHz Monopulse Tracking Radar*, NSWC/WOL TR-78-30, 10 March 1978.

APPENDIX A

MILLIMETER WAVE ACTIVE MONOPULSE RADAR TEST PLAN

APPENDIX A

MILLIMETER WAVE ACTIVE MONOPULSE RADAR TEST PLAN

OVERALL TEST PLAN OBJECTIVES

1. To determine radar capability to acquire, lock-on, and track a variety of surface and air targets and collect tracking data on such targets.

2. To measure side lobe and main lobe clutter, target cross-section, multipath scintillation, glint, track fluctuation, and system dynamic lag.

TEST PLAN OUTLINE

1. Initial Checkout on Static Target

   A. System Functional Checkout

   B. Target tracking data for a stationary and height adjustable surface target.

2. Surface Craft Target Tracking

   A. Surface Craft vs Range

   B. Clutter Effects (main lobe)

3. High Angle Tracking of Controlled Flying Target (Light Aircraft)

   A. Target Acquisition Problems

   B. Dynamic Lag

   C. Track Fluctuation

   D. Scintillation

   E. Glint

4. Low Angle Tracking of Controlled Flying Target (Light Aircraft)

   A. Multipath Effects (Az and El out vs range or angle)

   B. Clutter Effects (side lobe and main lobe off-axis)

5. Repeat Parts 3 and 4 with Military Aircraft

SYSTEM OUTPUT DATA COLLECTION FORMAT

1. Azimuth and Elevation Angle Channel Output Signal--Error signals are obtained from the video tape and TV monitor. Displacement of the track symbol on TV screen from boresight (center) represents the magnitude of azimuth and elevation error. TV camera is boresighted to radar line of sight, and it contains a visual image of the target.

2. Range to Target-- Range will be obtained from decimal digit output display. Display will be superimposed on the video camera image in 1 and therefore synchronized in time. This will be accomplished using split screen imaging with a second TV camera focused on the range display.

3. AGC Control Voltage or Log IF Amplifier Output Voltage--A calibrated conversion chart will be used to obtain the magnitude of the received signal (Σ channel return signal). This output will be coordinated in time with 1 and 2 above and recorded using the same camera as 2.

4. Sum Channel Video, Early Gate, and Both Angle Channel Outputs vs Time--These parameters will be synchronized in time and displayed on a four-channel oscilloscope. The sum channel video vs time or range is the A-scope. This output data will be used as an aid in the acquisition and tracking of the targets by the system operator. Position of the early gate with respect to sum channel video is an indication of system lock-on and tracking. This data is not recorded or synchronized in time with the video tape.

5. B-Scope Presentation of Range vs Azimuth Angle--This will be used to view target area and will not be recorded. It will be used as an acquisition aid by the operator.

6. Elevation Angle to Target--The elevation angle to the target will be presented on the display by use of a third TV camera and split screen TV imaging. This data will be synchronized with 1 and 2.

7. Date and Time of Test--The date and time of testing will be recorded on camera in 2 above.

DATA SHEET

Target Type--

Target Augmentation--

Target Speed--

Target Heading or Course--

Target Aspect--

Target Height--

Environment: background _____ sea state _____

wind speed _____ temperature _____

Date--

Time--

Run Number--

Video Tape Number--

Start Range--

End Range--

Transmitter Input Power at Antenna Terminals--

PRF--

Pulsewidth--

Comments--

DETAILED TEST PLAN

1. Initial Checkout on Static Targets

Objective: To perform initial system checkout and test basic radar tracking performance on a stationary target.

Approach:

A. A basic operational test of the radar will be made after mechanical installation of: radar/pedestal on tower, control console in tower house, power lines, electrical cables, signal lines, etc. All wiring connections and electronic assemblies will be checked initially before operating radar system.

B. A land mounted corner reflector will be used initially to check radar operation first in target acquisition and tracking and will then be used to boresight TV system. The corner reflector target will be positioned as far away from the radar as possible toward the water. This check will not require recording data, but will be a simple check to determine if all subsystems of the radar are operating properly and will not depend on scheduled targets. If the radar does not function properly, this target can be used to troubleshoot the radar.

C. If the radar is operating properly, the corner reflector may be moved around to determine if the radar will follow it.

D. An acquisition and tracking attempt of a distant stationary target should be performed.

E. A final measurement will involve an adjustable height corner reflector over water to obtain a multipath measurement. It may be more convenient to use a stationary boat for a platform.

Procedure:

A. Basic Operational Test

(1) Check all wire connections, cable connectors, etc., for proper location and connection. Check all mechanical connections.

(2) Turn pedestal control electronics on and check pedestal operation in all modes except Auto-Track.

(3) Pressurize waveguide system and turn transmitter main breaker on. A warm-up period of approximately 15 min is required before filament ready light is energized. Turn console power supplies to on position after filament ready comes on. Switch transmitter trigger switch to on position. Observe A-scope presentation for transmitter pulse at zero range. This is an indication of transmitter operation.

B. Stationary Corner Reflector Test: Position a corner reflector on land as far away from radar as possible (greater than 800 ft). A corner reflector at ground level is usable, but a corner reflector mounted on the tower located 300 yd from radar is more desirable. Acquire, lock-on, and track the corner reflector with the radar. Boresight the TV system and TV track symbols on the target center.

C. Moving Target Test: Move corner in B to determine if radar will follow target. Use video recorder to record data.

D. Distant Stationary Target: Select a distant stationary target and then acquire, lock-on and track it.

E. Adjustable Height Corner Reflector Over Water

(1) A corner reflector target capable of being adjusted in height over water is desirable to obtain a measurement of the multipath effect vs elevation angle (target height). If this target option is available, the following test can be run:

(a) Acquire and lock-on corner reflector suspended __ ft over water at a range of __.

(b) Slowly lower corner reflector and record Az and El error voltage vs target height.

(c) Lower corner reflector to point at which radar attempts to track corner reflector image.

2. Surface Target Tests

Objective: To perform surface target acquisition and tracking and collect tracking data.

Approach:

A. Patrol boats are known to frequent the test site area. If no targets are scheduled, a track attempt on a target of opportunity could be tried, so that test personnel can become familiar with the mechanics of radar operation. It will be necessary to determine if the patrol boat can be seen by the radar without augmentation by a corner reflector, and if a moving patrol boat can be acquired and tracked easily.

B. It may only be possible to conduct the tests using a cooperative scheduled patrol boat due to acquisition and lock-on problems. Testing should start with an acquisition and tracking attempt of a patrol boat at rest. The patrol boat may need to be augmented with a corner reflector if its cross section is not sufficiently large with respect to the target background.

Tests with a moving patrol boat will follow. This will include acquisition and tracking of a patrol boat crossing target (beam aspect) at slow and fast speeds. Track lag can be measured and the effects of background main lobe clutter can be observed. A patrol boat moving toward and away from the radar may be an easier moving target to acquire and lock-on. If it has been found necessary to augment the patrol boat with a corner reflector, it would be beneficial to vary the height of the corner reflector and measure multipath effects. Target range and target height will be determined from calculations. The magnitude of the multipath effects can be measured by recording Az and El tracking errors vs target height. If this test was performed in the stationary target tests, it is not necessary to repeat it here.

Procedure:

A. Preliminary Surface Target Tests

(1) An initial test will be to attempt acquisition, lock-on, and track of a surface target. A scheduled patrol boat that is stationary would be the most desirable target. If the radar is unable to acquire, lock-on, and track this target, the radar return signal is not adequate and will require enhancement with a corner reflector.

(2) If in 1 the radar is unable to acquire, lock-on, and track the patrol boats, install the corner reflector and orient it for maximum return on beam aspect. Attempt acquisition, lock-on, and track of augmented stationary target.

(3) Attempt acquisition, lock-on, and track of augmented moving target. (Crossing target course with motion perpendicular to line of sight to radar.)

B. Surface Target Tests with Scheduled Targets

(1) Attempt acquisition, lock-on, and tracking of a stationary patrol boat (beam aspect). Record data after achieving a tracking condition.

(2) Attempt acquisition, lock-on, and tracking of a maneuvering patrol boat. Record all data.

(a) Beam Aspect, Crossing Target Path with course perpendicular to line of sight of radar.

(b) Bow Aspect, Radial Target path with course radially approaching radar.

(c) Stern Aspect, Radial Target path with course radially away from radar. [Make as many runs as possible (a), (b), and (c) in allotted time.]

(3) Perform multipath measurement as follows:

(a) With patrol boat stationary and corner reflector mounted such that it can be raised or lowered in height, acquire, lock-on and track corner reflector in its highest position.

(b) Slowly lower corner reflector and record Az and El error channels vs target height.

3. High Flying Aircraft Tests

Objective: To attempt acquisition and tracking of a high flying target and collect tracking data.

Approach:

A. It is doubtful that acquisition and track can be obtained of most noncooperative air targets. Since the test site is a restricted air space, noncooperative air targets of opportunity will probably not be available.

B. For cooperative scheduled air targets, the flight path should initially be moving on a radial racetrack course toward and away from radar. This flight path should be the easiest to acquire and track. The data from this run will show the radar tracking performance as well as the target signatures for the high flying target. Other target courses recommended are a crossing target racetrack course (perpendicular to the line of sight to the radar) and serpentine course radially in toward the radar.

Procedure: Acquire, lock-on, and track the aircraft for the target courses described in the approach. There may be some difficulty in acquiring the small target cross-section. The straight line radial course is the easiest course to acquire and should be attempted first. Record target courses and target type in addition to video tape data.

For the cooperative target, three basic target courses are recommended:

A. Racetrack course straight away from and straight toward radar (radial course).

B. Racetrack course pattern perpendicular to line of sight of radar (crossing target simulation).

C. Serpentine maneuvering course toward radar.

Ranges and length of racetrack courses will be determined by calculation. High and low speed targets are recommended.

4. Low Flying Aircraft Tests

Objective: To attempt acquisition and tracking of a low flying target and measure the multipath error vs range.

Approach:

A. A low flying target will most likely be a cooperative target. The flight path of the target should be a radial racetrack course with target moving toward and away from radar. This flight path will be the easiest to acquire and track. The important target parameters are target height, velocity, target type, path outline, in addition to the video tape recorded data. This data will show the tracking performance for a low flying target and as a result the low grazing angles will yield a multipath measurement.

B. A second target course pattern would be the racetrack course perpendicular to the line of sight to the radar. Both low and high speed targets would be desired here.

Procedure:

A. Acquire, lock-on, and track the aircraft for the radial racetrack course. It will probably be necessary to perform the initial acquire, lock-on, and track with the target heading away from the radar and at its closest point to the radar. This is due to the magnitude of the multipath error for small elevation angles. The radar may not be able to switch to angle track mode with such a large angle error output that results from the multipath. Data recorders should be operating with the aircraft heading away from the radar.

B. Acquire, lock-on, and track the aircraft using the second target course pattern with both low and high speeds.

5. Military Aircraft Tests: Repeat 3 and 4 with military aircraft.

Table A-1. Radiation Hazard Distances

Transmitter Power, Peak (W)	Transmitter Power, Average (W)	Attenuator Setting (dB)	Safe Radius for Less Than 10 mW/cm^2 (ft)	Safe Radius for Less Than 1 mW/cm^2 (ft)
100K	55	0	185	483
10K	5.5	10	57	153
1K	.55	20	No Hazard > 10 mW/cm^2	57
100	.055	30	No Hazard > 10 mW/cm^2	No Hazard > 1 mW/cm^2
10	.0055	40	No Hazard > 10 mW/cm^2	No Hazard > 1 mW/cm^2

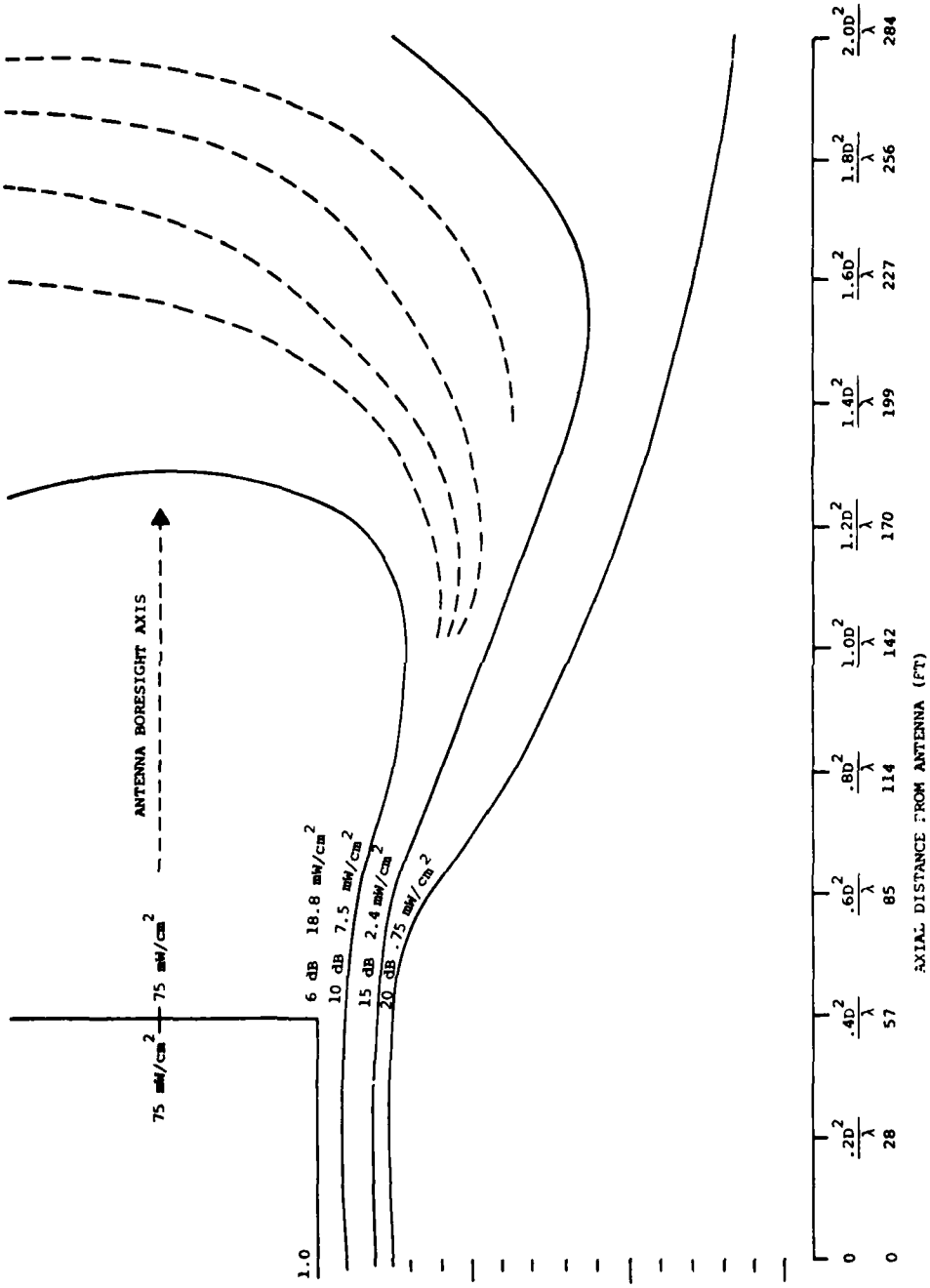

Figure A-1. Power Density Contours at Full Power (100 kW Peak)

TEST SCHEDULE PLAN

The entire test program will require 14 days. Approximately two tests will be scheduled per week depending on range availability and set up time for each test. The number of tests per week as well as the actual calendar day on which each test will take place will remain flexible. This will depend on range scheduling, target availability, weather, and operational condition of test radar.

Each day of testing will require two test personnel on tower and the necessary additional personnel from test range to coordinate and pilot targets. A 1-day test will contain many tracking runs for one or more target types.

Quick looks at the data will take place during tests. Preliminary data reduction and analysis are expected to take place on those days when tests are not in progress. Further data reduction and final report writing will be performed for 3 months following completion of all tests. This will be a 4.4 man month effort.

The radar must be off the main tower range by 31 March 1979. The radar will be moved to another location before this time. A suggested location is the White Oak Laboratory where the radar could be set up to track the numerous air targets of opportunity at this site.

A cost estimate for the testing per test will be determined as follows: based on one test per day with two test personnel at a cost of $200.00 per person per day and use of test range facilities including manpower to run targets at a cost of $1,000.00 per day, the total cost per test per day will be approximately $1,400.00.

Table A-2. Test Schedule

	1st Week	2nd Week	3rd Week	4th Week	5th Week	6th Week	7th Week
Initial Checkout on Static Target	▨						
Surface Craft Target Tracking		▨					
High Angle Tracking of Controlled Flying Target (Light Aircraft)			▨	▨			
Low Angle Tracking of Controlled Flying Target (Light Aircraft)					▨	▨	
High and Low Angle Tracking of Controlled Flying Target (Military Aircraft)							▨

*Total test program consists of 14 days of testing with 2 test days per week.

DISTRIBUTION

	Copies
Chief of Naval Research Attn; ONR-715 800 N. Quincy Street Arlington, VA 22217	2
Commander Naval Sea Systems Command Attn: SEA-62R, B. Blaine SEA-62R, C. Jedrey SEA-62R, R. Muir SEA-62X, R. Desselle SEA-62Y, J. Carroll Naval Sea Systems Command Headquarters Washington, DC 20362	1 2 2 2 2
Commander Naval Air Systems Command Attn: NAIR-360, J Willis NAIR-360, J. Malloy Naval Air Systems Command Headquarters Washington, DC 20361	1 1
Commander Naval Electronic Systems Command Attn: NELEX-034, B. Walpole Naval Electronic Systems Command Headquarters Washington, DC 20360	2
Commanding Officer Naval Research Laboratory Attn: Library 4555 Overlook Ave., SW Washington, DC 20375	1
Commander Naval Weapons Center Attn: Library China Lake, CA 93555	1
Commander Harry Diamond Laboratories Attn: Library Adelphi, MD 20783	1
Department of the Air Force Ballistic Missile Office Attn: Library Norton AFB, CA 92409	1
Director Defense Advanced Research Projects Agency Attn: N. J. Willis 1400 Wilson Boulevard Arlington, VA 22209	2
Defense Technical Information Center Cameron Station Alexandria, VA 22314	12